

Phenomenological approach to XANES data analysis:

Shortcuts to understand local
structure and chemistry from XANES
spectra

Carlo Meneghini

carlo.meneghini@uniroma3.it

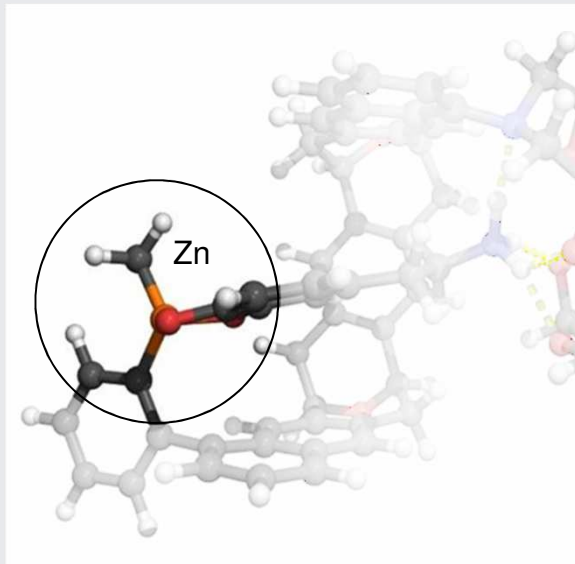
<http://host.uniroma3.it/docenti/meneghini/index.html>



XIV School on Synchrotron Radiation:
Fundamentals, Methods and Applications
Muggia, Italy / 18-29 September 2017



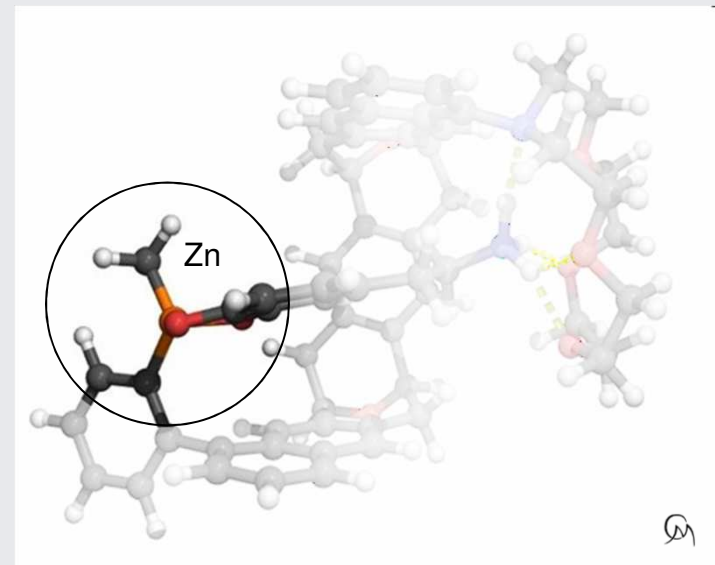
XAFS is a local sensitive, chemical selective probe which may provide **structural**, **electronic** and even **magnetic** (XMCD) details

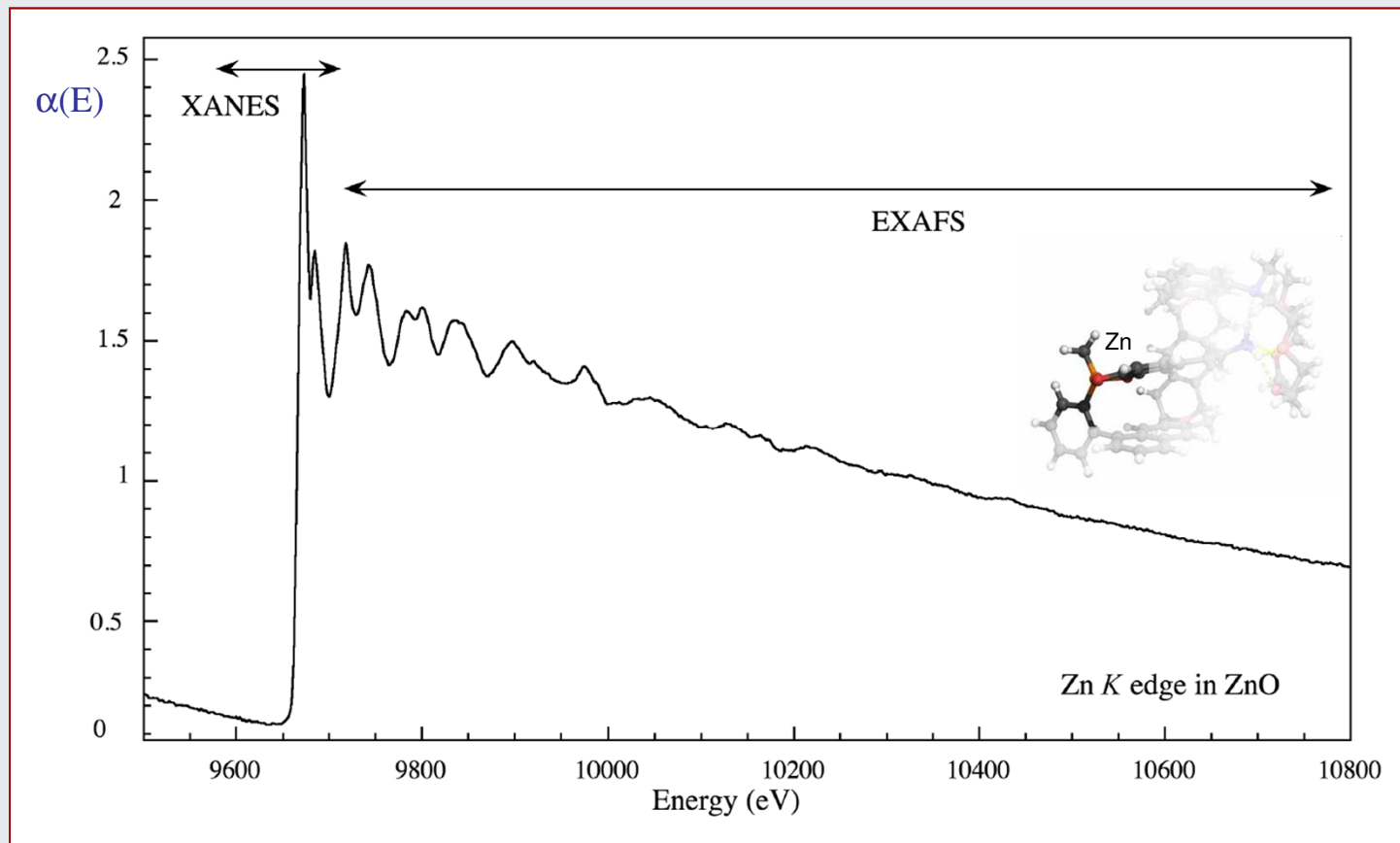


Subjective (Absorber) view of the local atomic structure in your sample

XAFS is a local sensitive, chemical selective probe which may provide **structural**, **electronic** and even **magnetic** (XMCD) details

- Applicable to materials in any aggregation state: **gas, liquid, solid, single crystals, powders, amorphous, nanostructures, etc....**
- Measurable from **bulk** to the highest **diluted** samples (micro-molar)
- Versatile probe (**bulk, surfaces, layered structures, quantum structures, etc...**)
- Simple experimental set-up and easy data collection
- Fast (quick XAFS) and ultrafast (dispersive) data collection
- Directional sensitivity (polarized XAS): to probe **structural anisotropy**
- Element selective Magnetic state sensitive (XMCD)





EXAFS region: simple analytical formula suited for data fitting and *easy* structural refinement

$$\chi(k) = \frac{1}{k} \sum_j A_j(k, r_j) \sin(2kr_j + \psi_j(k))$$



$$A_j(k, r_j) = S_o^2 \frac{N_j}{r_j^2} |f_j(k, r)| e^{-2k^2\sigma_j^2} e^{-2r_j/\lambda}$$

XANES region:

Hard theory

lack of an analytical expression

long computation time



Applications of XANES spectroscopy systematically increases

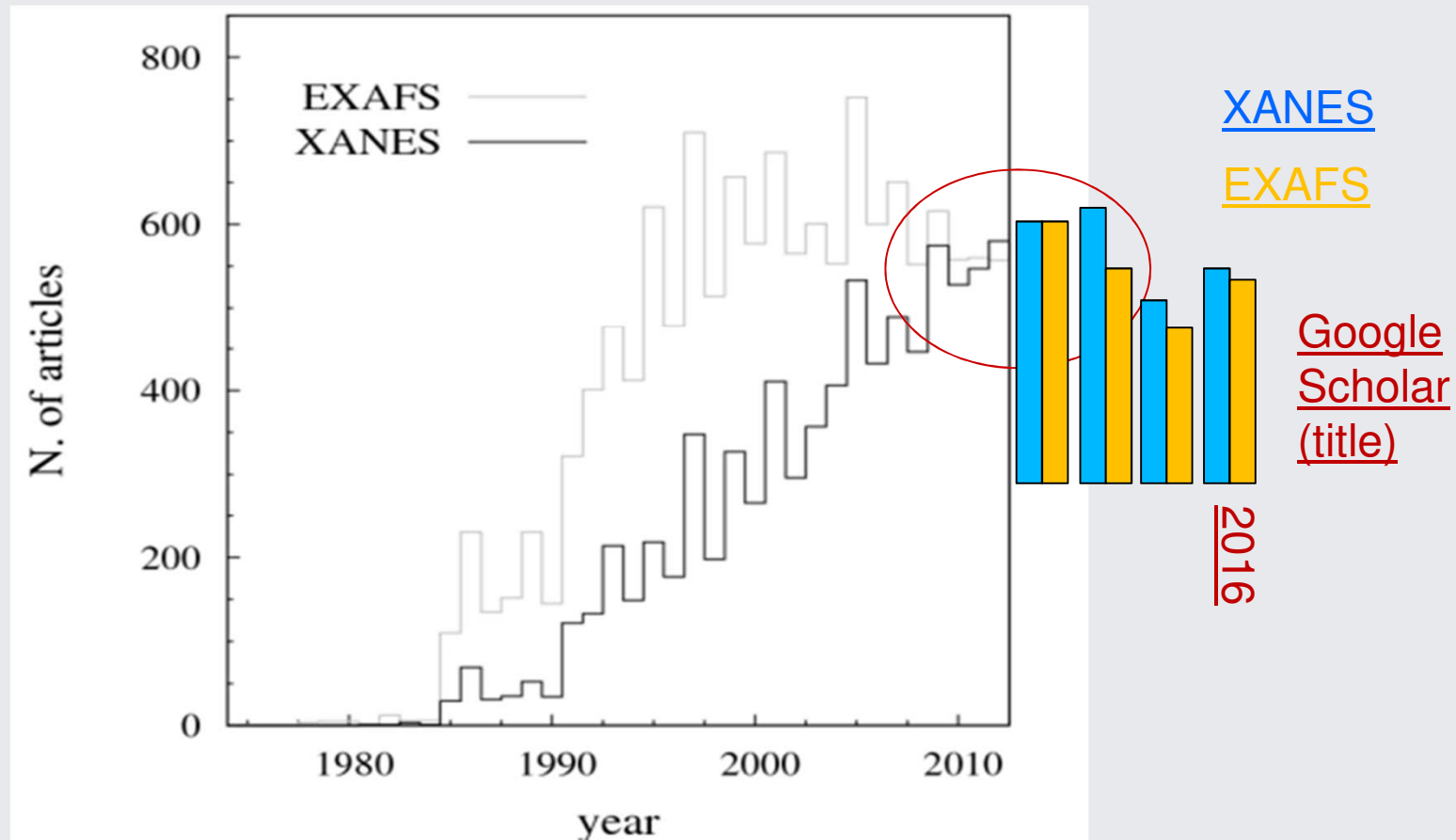


Fig. 1. Results of database search on ISI-web of knowledge using “EXAFS” (“XANES”) in *Topic* or *Title* fields.

XANES based probes: valuable advantages

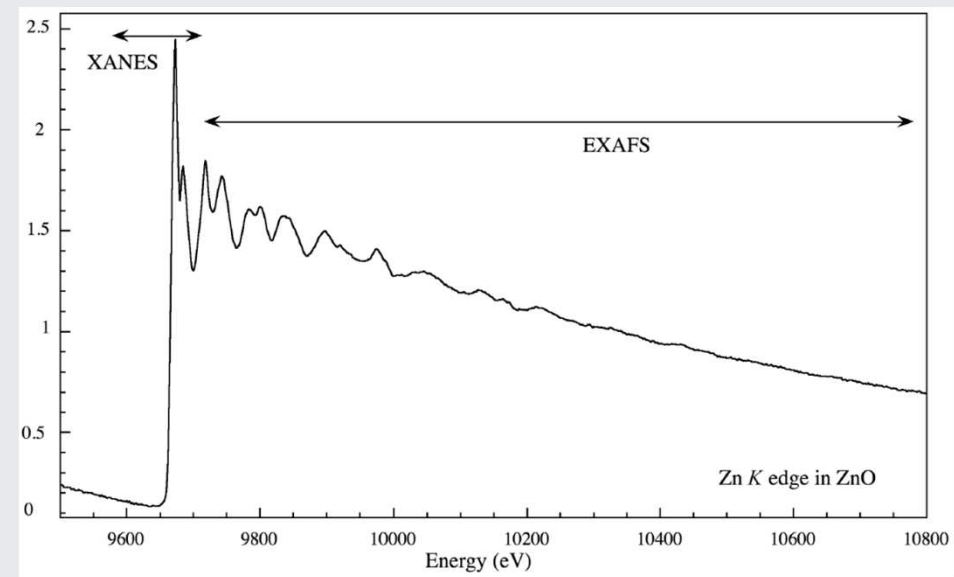
XANES signal is stronger than EXAFS

Damping of XANES signal due to structural disorder is weak

Electronic structure (DoS) and structural topology

Restricted energy range

May provide Chemical selective
Magnetic information (XMCD)



XANES signal is dense of electronic, magnetic and structural details

XANES signal is stronger than EXAFS:

- less sensitive to data statistics, sample quality, beam intensity,
- can be measured on less concentrated samples,
- can be measured faster than EXAFS (time resolved experiments),
- can be measured at low energies (i.e. Carbon, Oxygen, Nitrogen K-edges).

Damping of XANES signal due to structural disorder is weak:

- Applications to extreme condition studies: High **T**, High **P**, High **H**....

Electronic structure (DoS) and structural topology:

- XANES features are specially sensitive to the valence state, coordination chemistry, ligand symmetry of the absorber.
- Can be used as fingerprint for chemical speciation in mixtures and inhomogeneous systems.

Restricted energy range around the edge:

- Measurements at low energies (i.e. Carbon, Oxygen, Nitrogen K-edges)
- Fast data collection (time resolved XAS)
- XANES Microprobes (mapping) with sub-micrometer resolution

Chemical selective Magnetic information

- X ray Magnetic Circular Dichroism (XMCD) signal is an element specific probe for magnetism
- Sum rules at $L_{2,3}$ edges allow distinguishing orbital and spin contributions to the magnetic moment of the photoabsorber

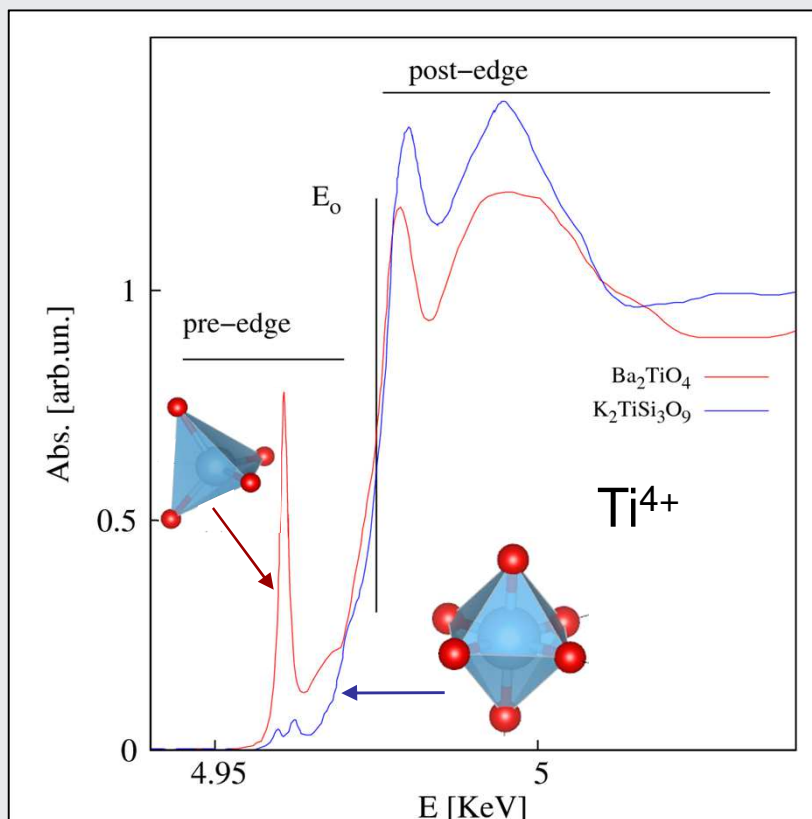
XANES theory
is complex



XANES are prone to
simple interpretation
for simple and fast
(semi-)quantitative
analysis

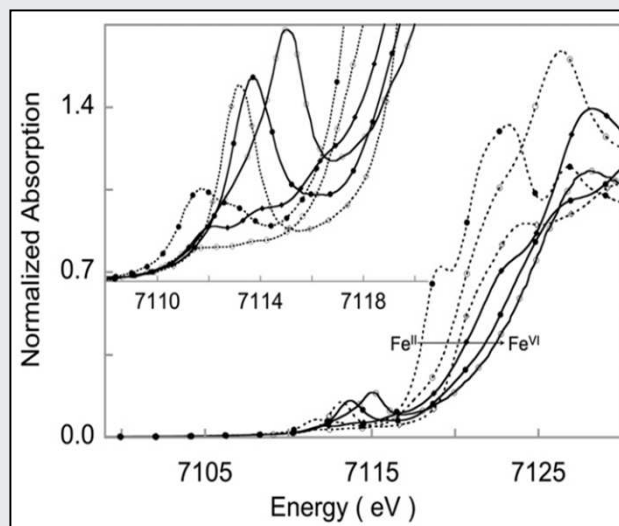


Deeper insight into the XANES region



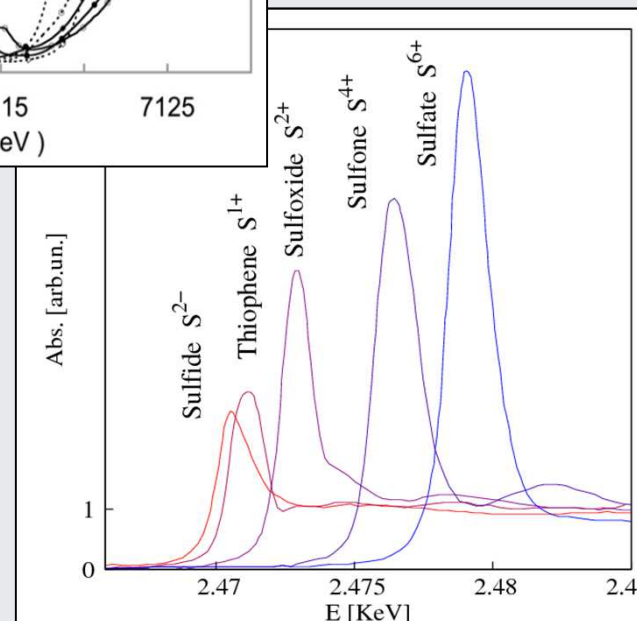
Local symmetry and XANES in Ti^{4+} compounds

XANES features are strongly related to the coordination geometry: coordination number and ligand symmetry



Fe K edges: representative XANES Fe in complexes

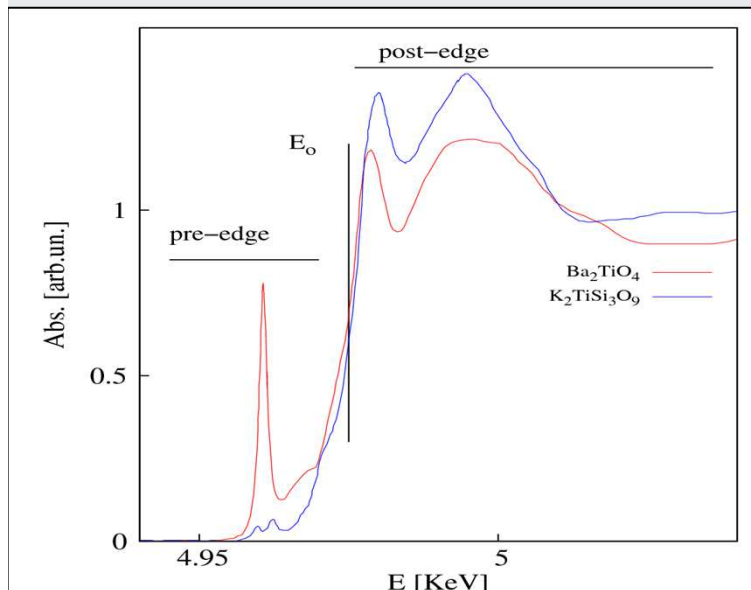
R. Sarangi, Coord. Chem. Rev. 257 459–472 (2013)



Sulphur K edges: chemical shift as a function of valence state of S-ions

Absorption Edges (energy position and shape) definitively depend on the oxidation state of the absorber

Origin of the XANES features



Pre-edge

caused by electronic transitions (mainly dipole allowed) to empty bound states near the Fermi level.

Provide information about absorber local geometry and electronic state around the absorber: number of neighbours, ligand symmetry, valence state

Edge (E_0) defines the onset of continuous states (not the Fermi level !)

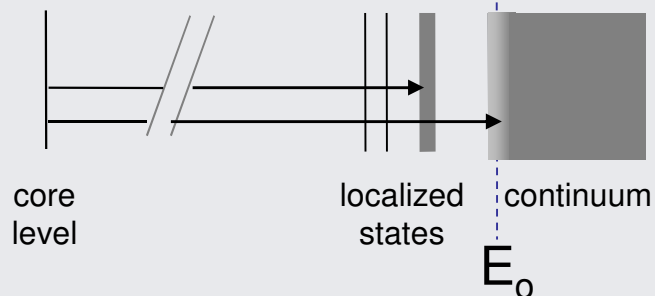
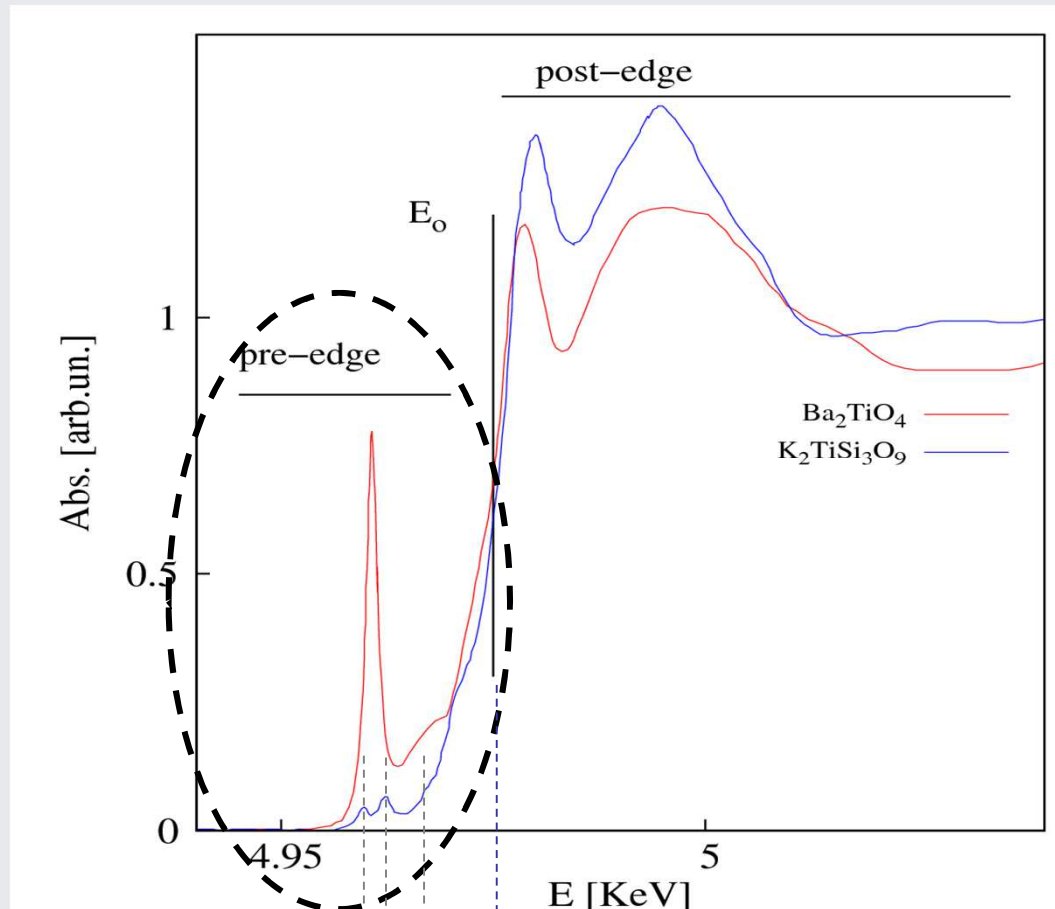
E_0 is a function of the absorber oxidation state & binding geometry. It may also increase by several eV per oxidation unit

Post-edge (XANES)

multiple scattering features (FMS)

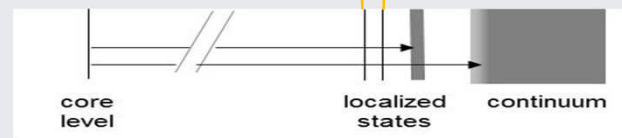
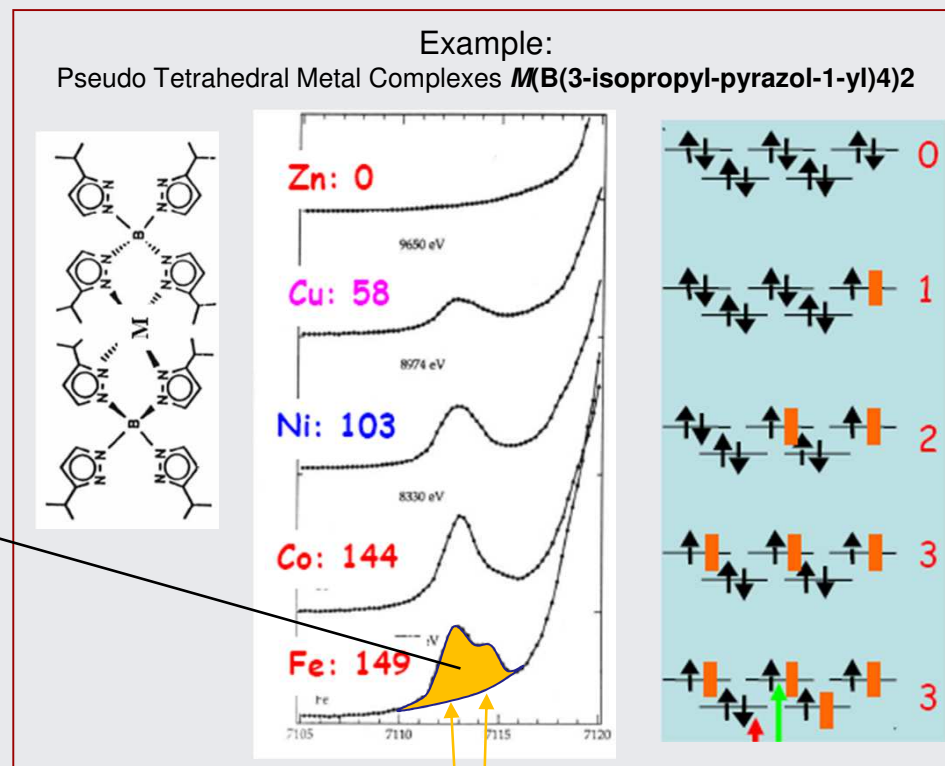
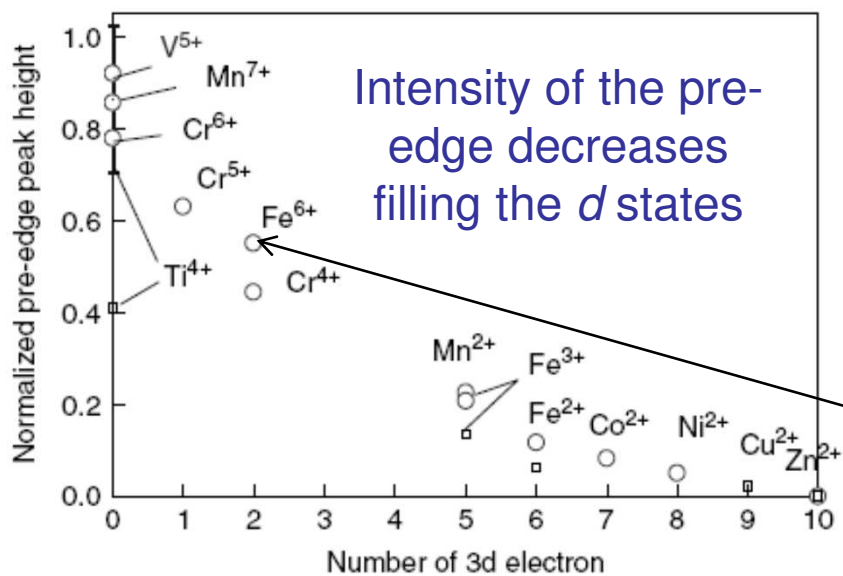
The analysis may provide finest details about local atomic structure and geometry.

The Pre-edge region



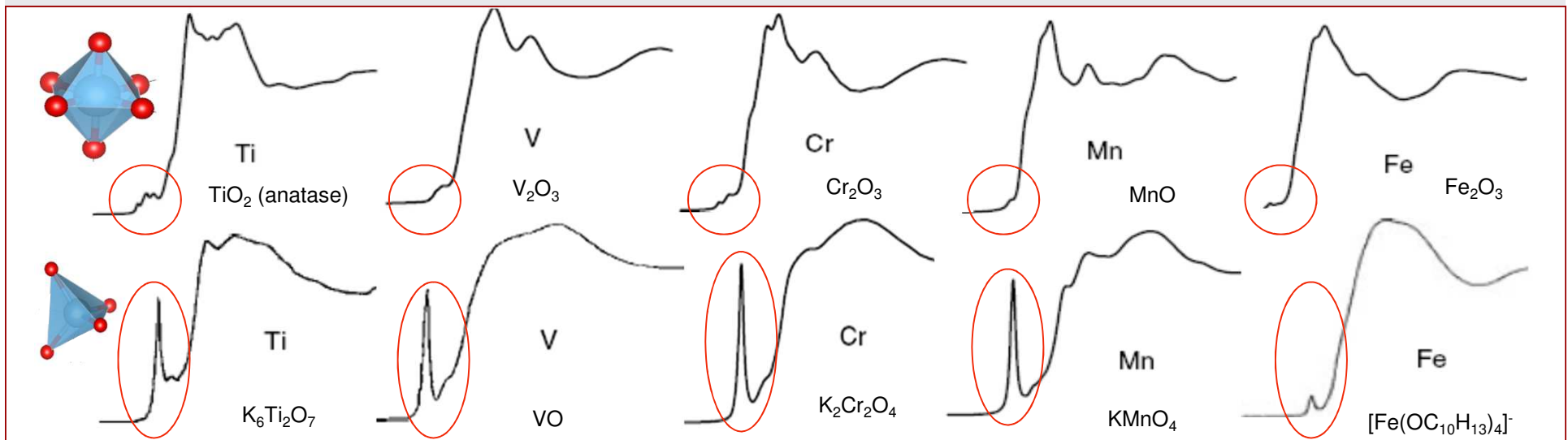
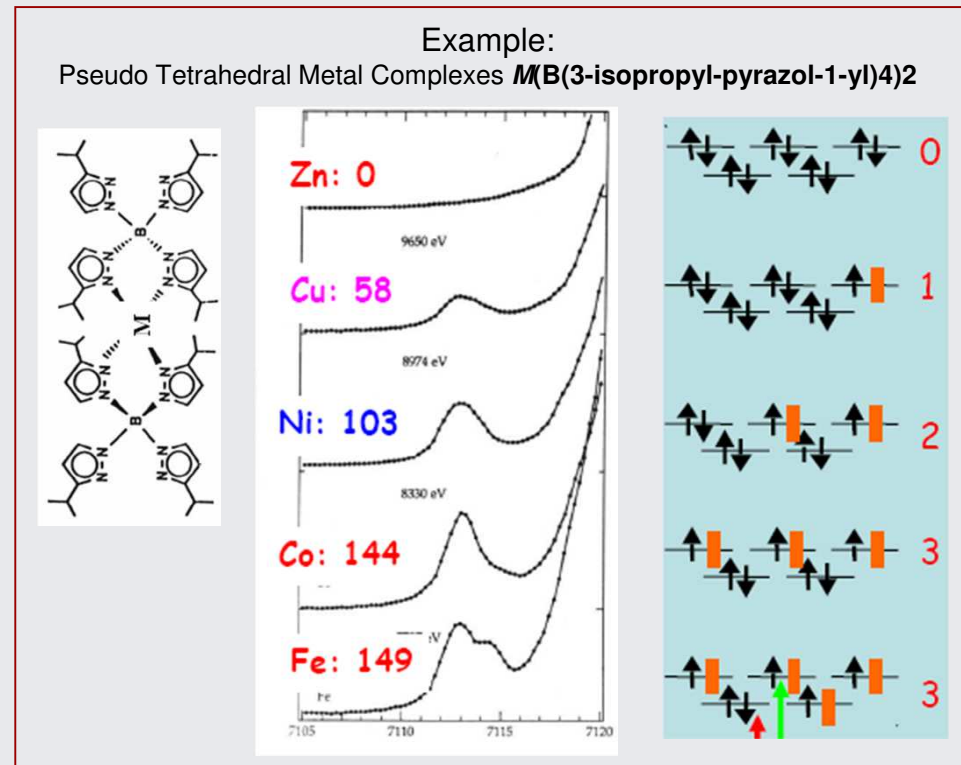
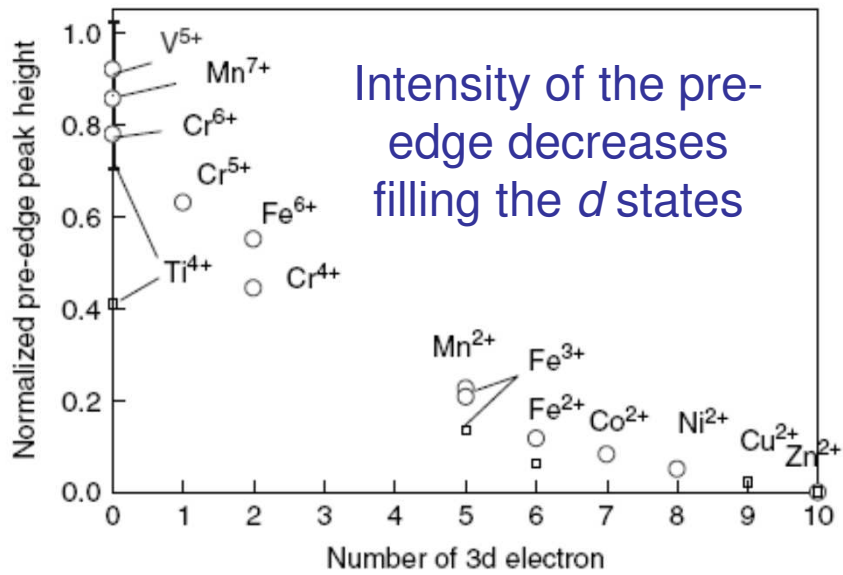
caused by electronic transitions (mainly dipole) to empty bound states near the Fermi level.

K edges of 3d metal oxide: intensity vs empty states

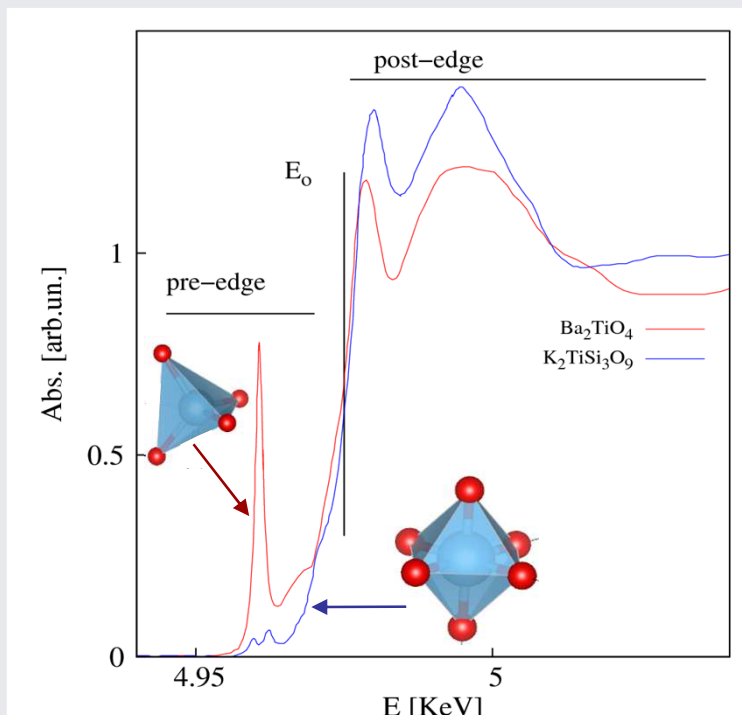


Pre-edge caused by electronic transitions (mainly dipole) to empty bound states near the Fermi level.

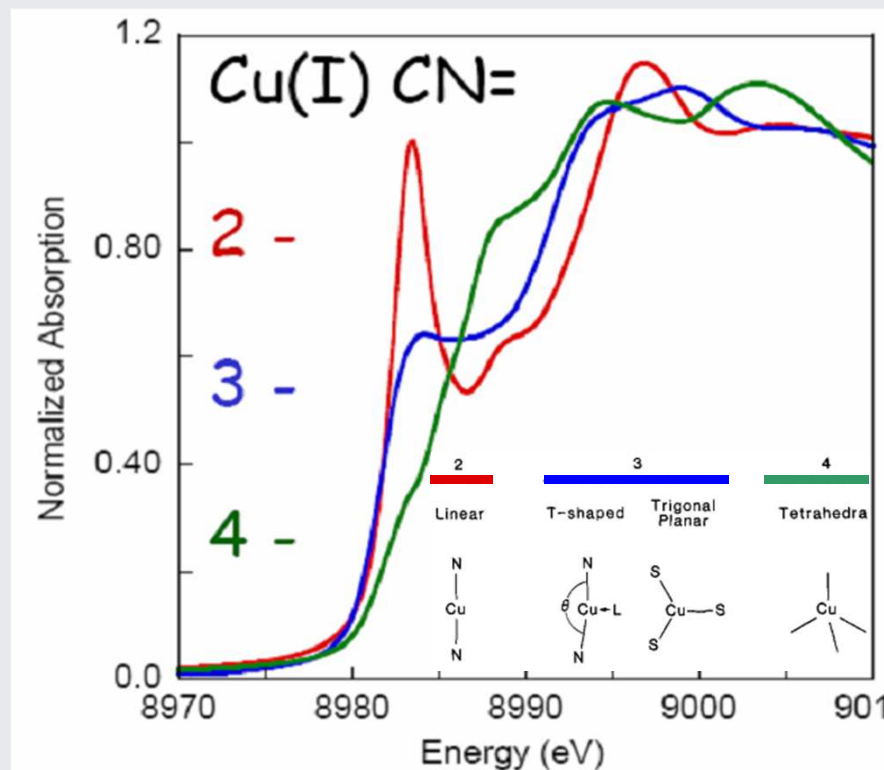
K edges of 3d metal oxide: intensity vs empty states



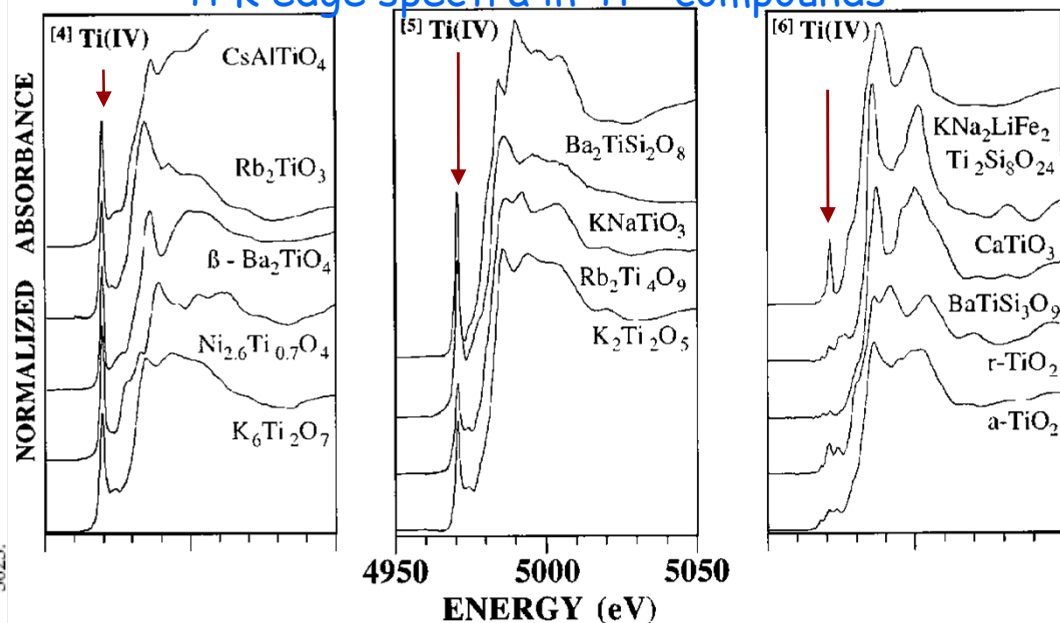
Pre-edge: sharp features signal the transitions to bound electronic levels below the continuum threshold



The XANES of the same ions, even in the same oxidation state, may behave definitively different in different compounds!



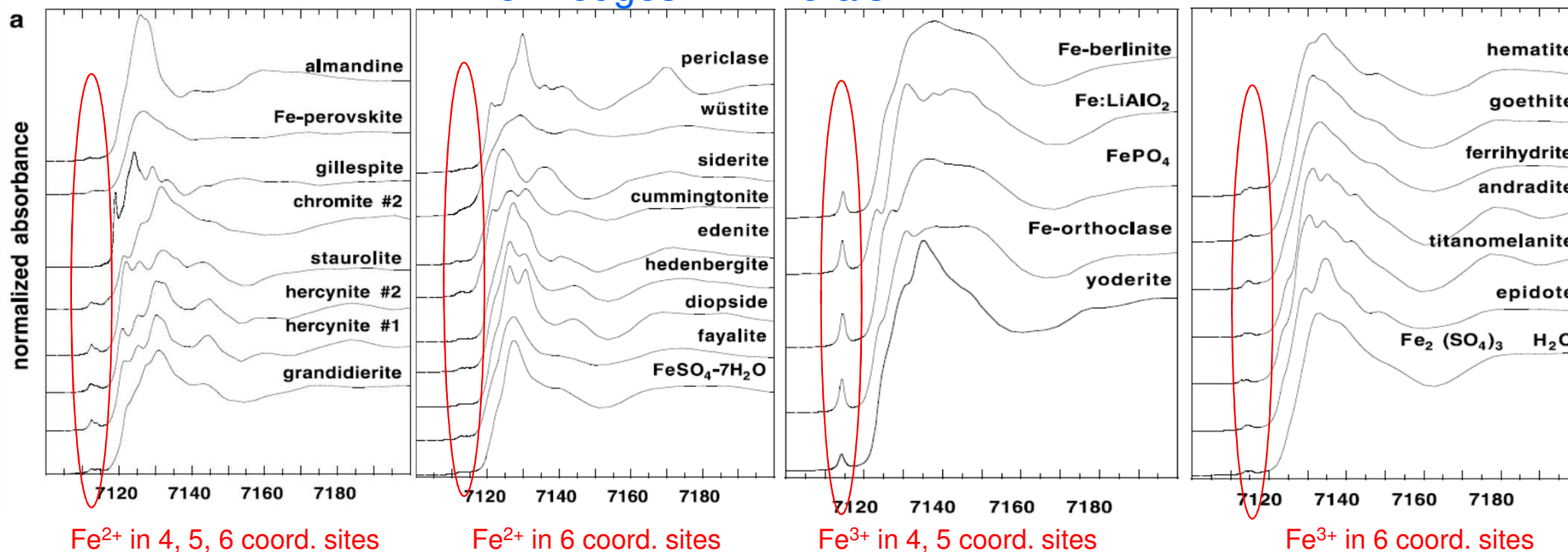
Ti K edge spectra in Ti⁴⁺ compounds



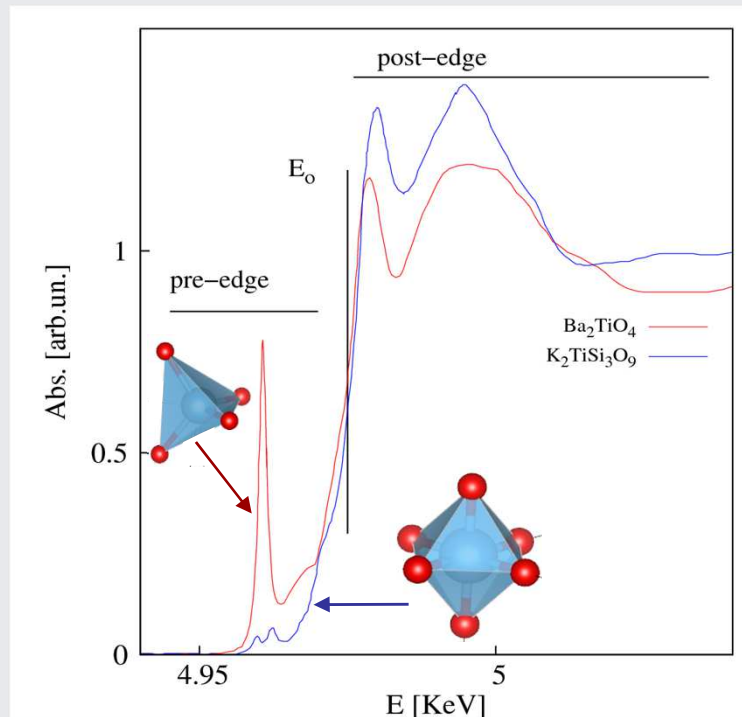
Ti K pre-edge peak in 4-, 5- and 6-fold coordinated Ti⁴⁺ compounds occurs at different energies and have different height/area

Fe K pre-edge looks definitely different as a function of Fe oxidation state and coordination number

Fe K edges in minerals



Pre-edge: sharp features signal the transitions to bound electronic levels below the continuum threshold



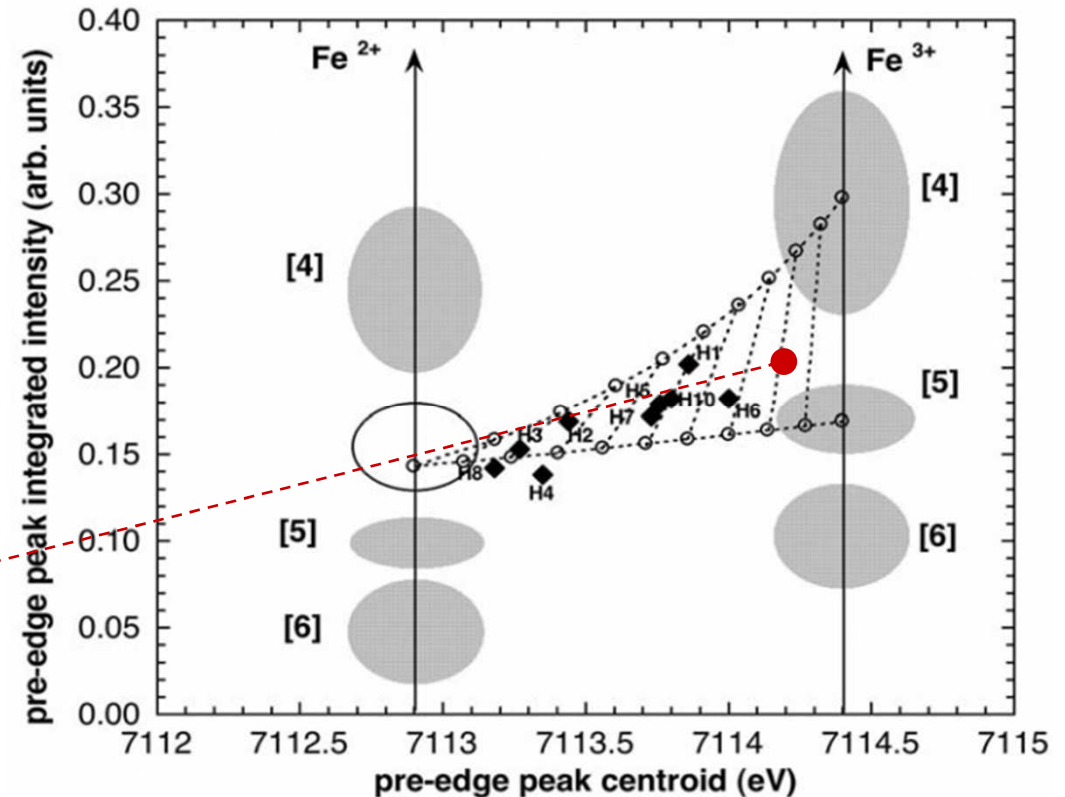
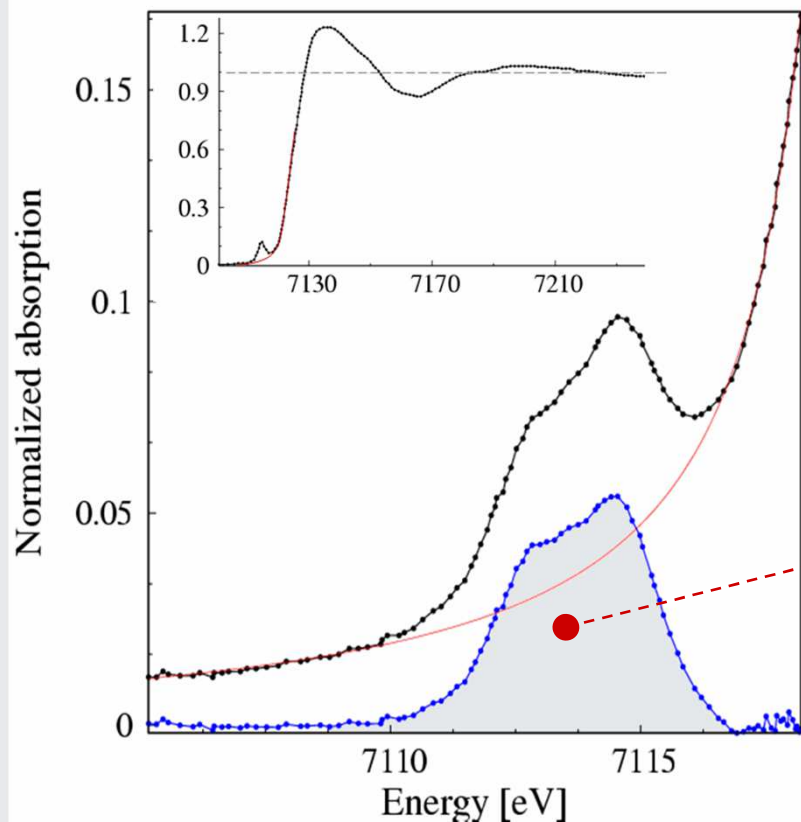
The XANES of the same ions, even in the same oxidation state, may behave definitively different in different compounds!

Quantitative Models: multiplet theory

Semi-quantitative approaches:

- Comparison with model compounds
- Molecular orbital symmetry (group theory)

The case of Fe: average valence and coordination from the pre-edge peak shape



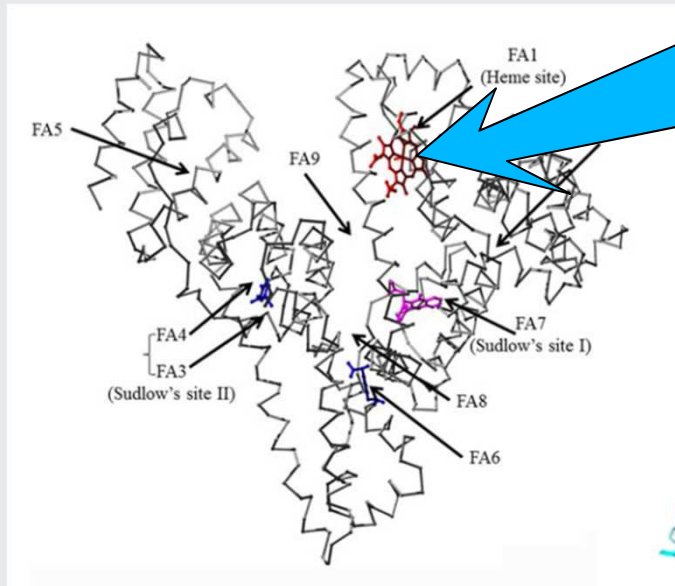
G. Giuli et Al. *Meteoritics & Planetary Science* 40, Nr 11, 1575–1580 (2005)

Pre-edge peak area vs position is related to valence state and coordination number of Fe absorbers

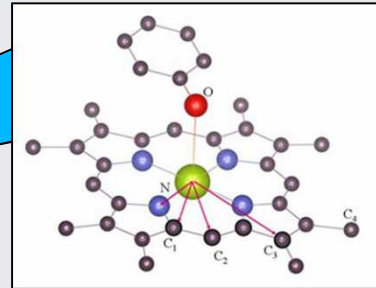
From Fe K pre-edge centroid position and peak area it is possible to individuate the average Fe valence state and coordination number

The case of Fe:

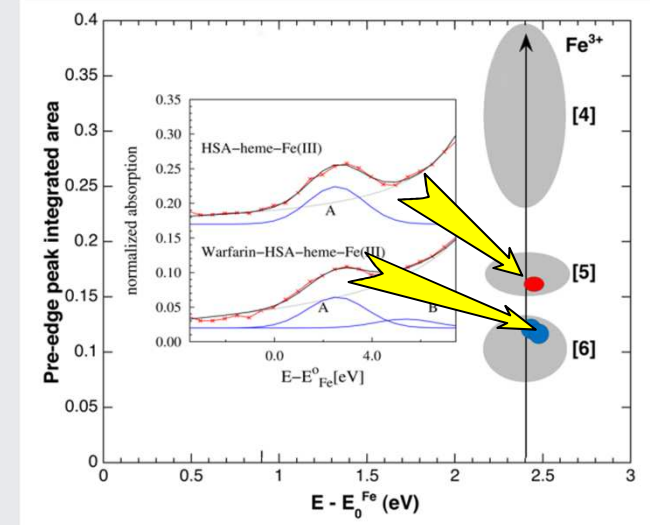
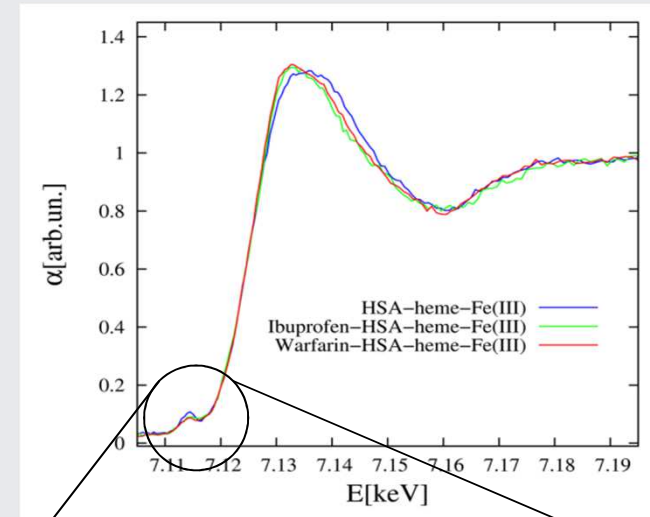
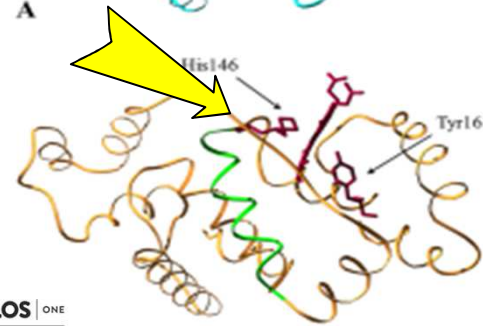
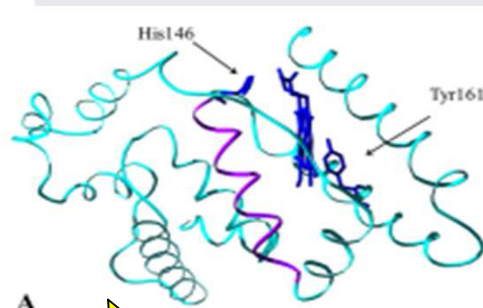
Ibuprofen/warfarin induce V to VI Fe coordination transition in HSA



Human Serum Albumin



Heme (Fe) site



OPEN ACCESS Freely available online

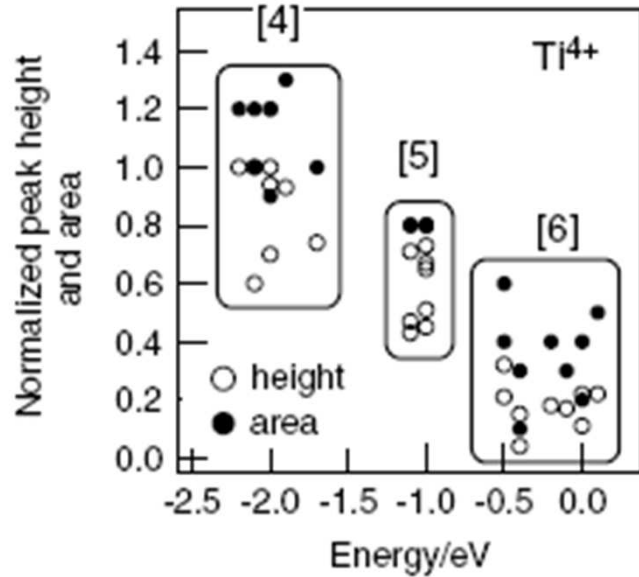
PLOS ONE

The Five-To-Six-Coordination Transition of Ferric Human Serum Heme-Albumin Is Allosterically-Modulated by Ibuprofen and Warfarin: A Combined XAS and MD Study

Carlo Meneghini^{1,2}, Loris Leboffe^{1,2,3}, Monica Bionducci¹, Gabriella Fanali³, Massimiliano Meli⁴, Giorgio Colombo⁴, Mauro Fasano³, Paolo Ascenzi^{2,5*}, Settimio Mobilio¹

...and Ti, V, ...: average valence and coordination from the pre-edge peak shape

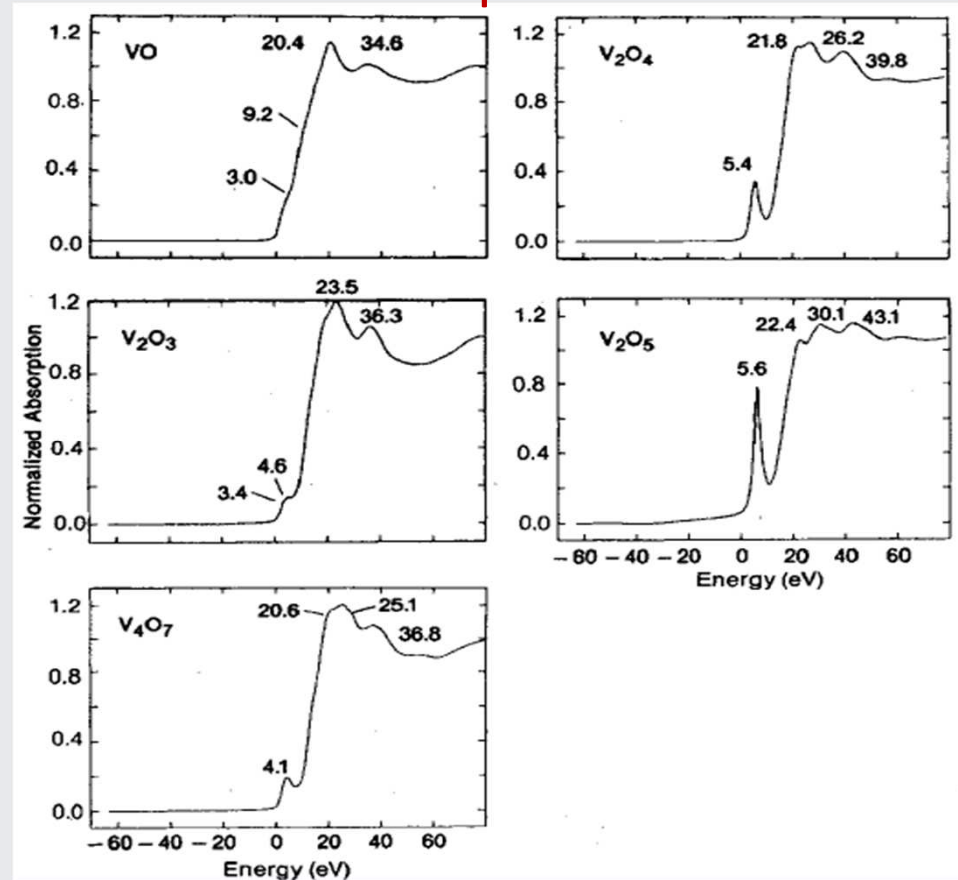
Ti⁴⁺ compounds



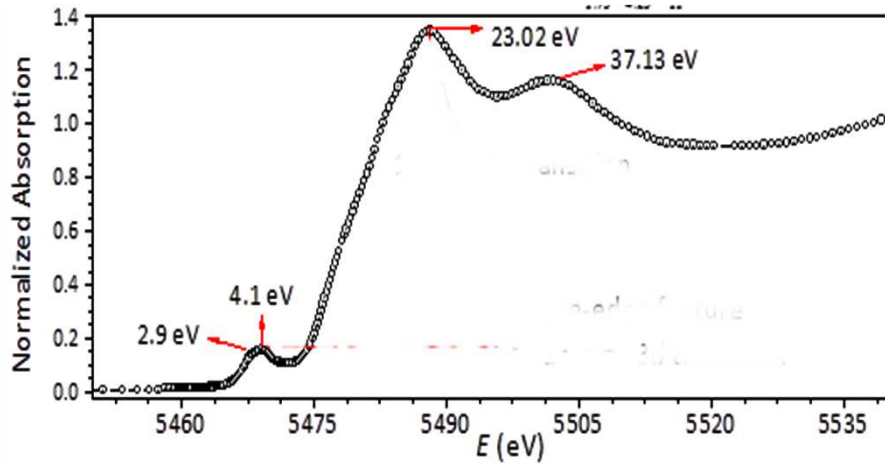
Ti pre-edge main peak intensity and area as a function of coordination number

6. Farges F, Brown GE, Rehr JJ. *Geochim. Cosmochim. Acta* 1996; 60: 3023.

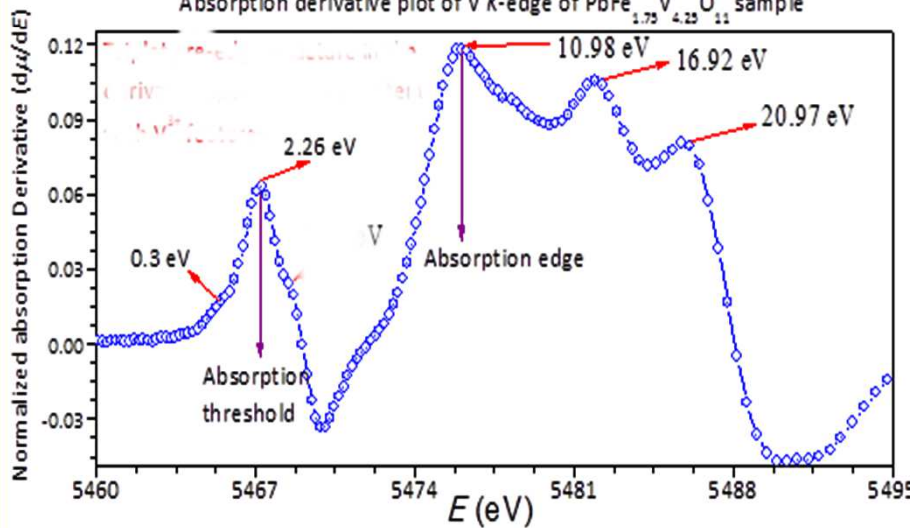
V compounds



It is possible to understand the absorber coordination looking at the intensity/area of pre-edge peaks in comparison with reference compounds data

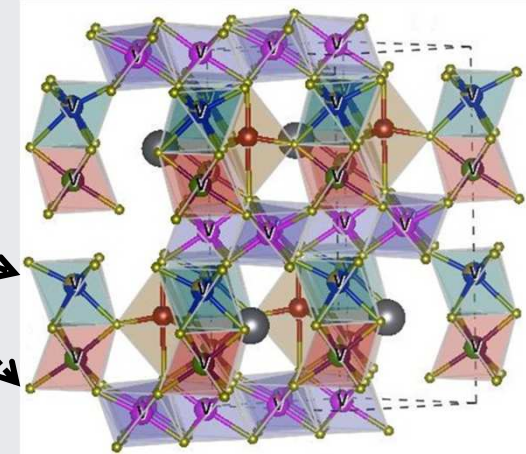


Absorption derivative plot of V K-edge of $\text{PbFe}_{1.75}\text{V}_{4.25}\text{O}_{11}$ sample

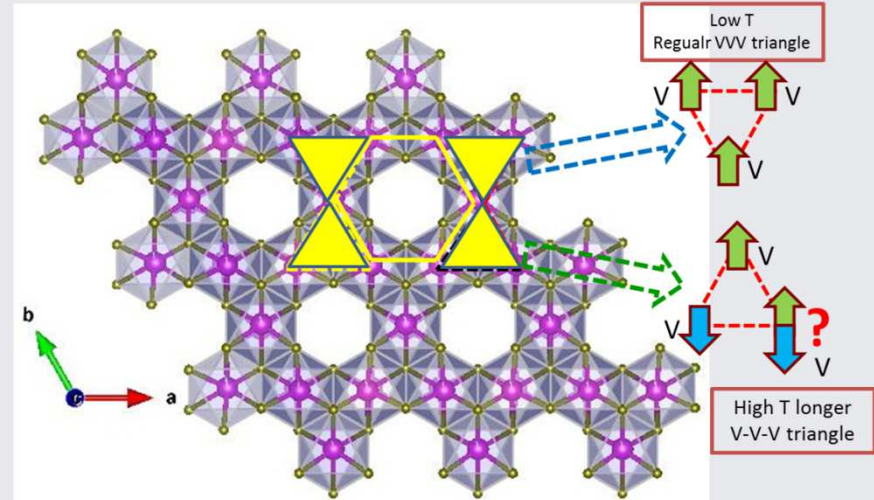


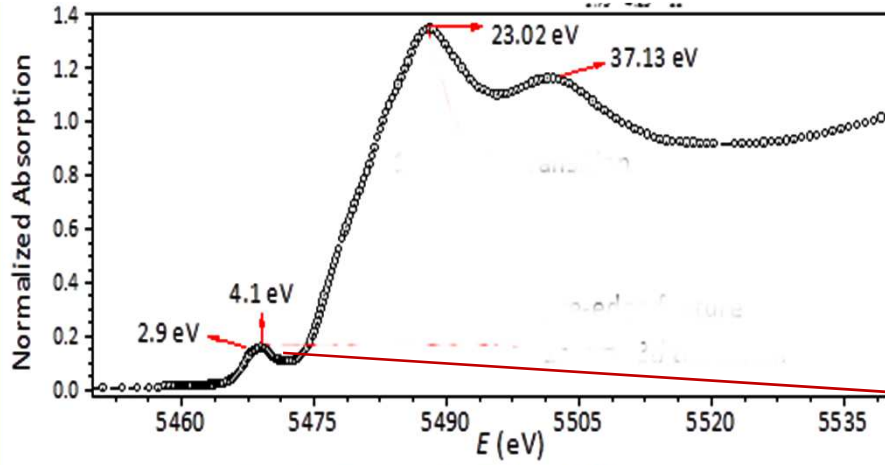
V-valence state

FeVO_9 dimer
having mixed
 $\text{Fe}^{3+}/\text{V}^{4+}$
occupancy

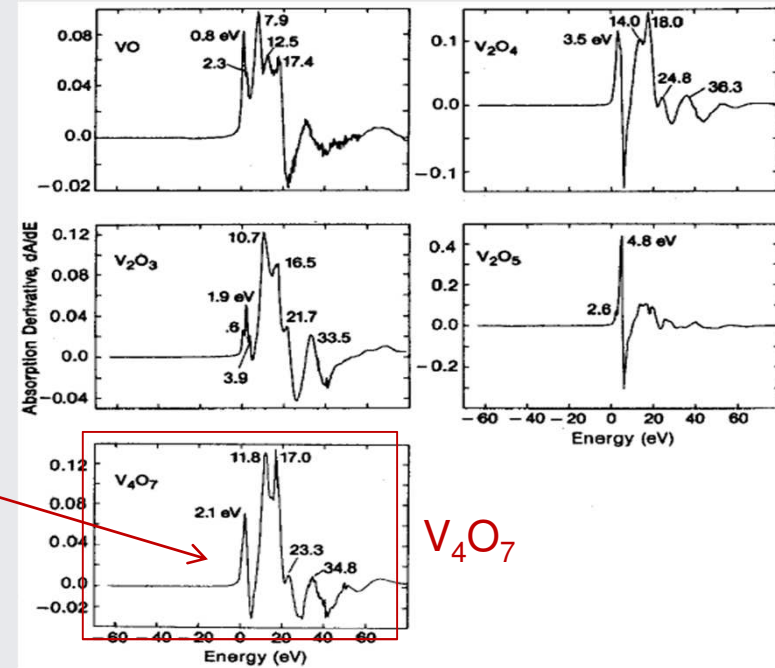
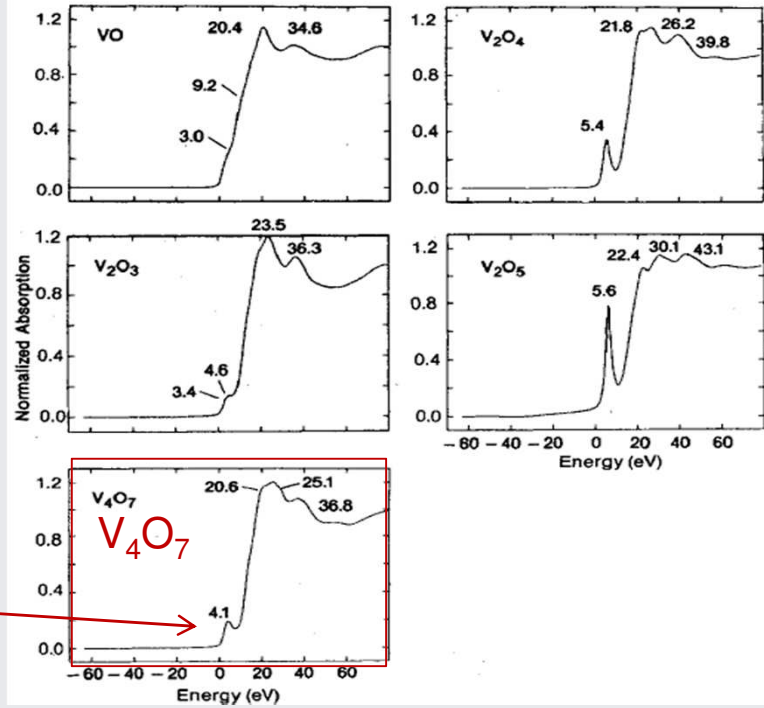
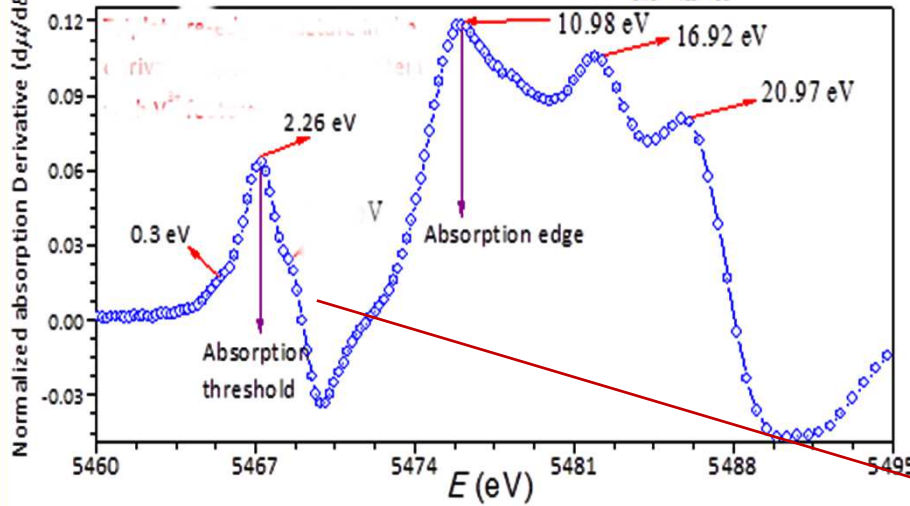


Formation of *kagome trimer* in the *a-b* plane



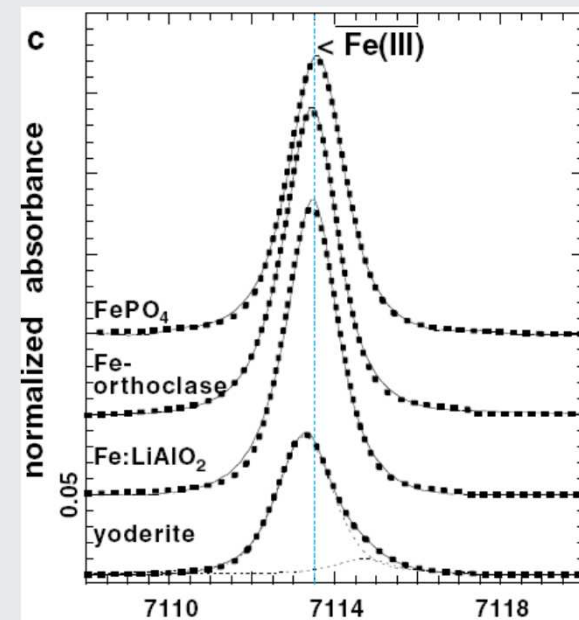
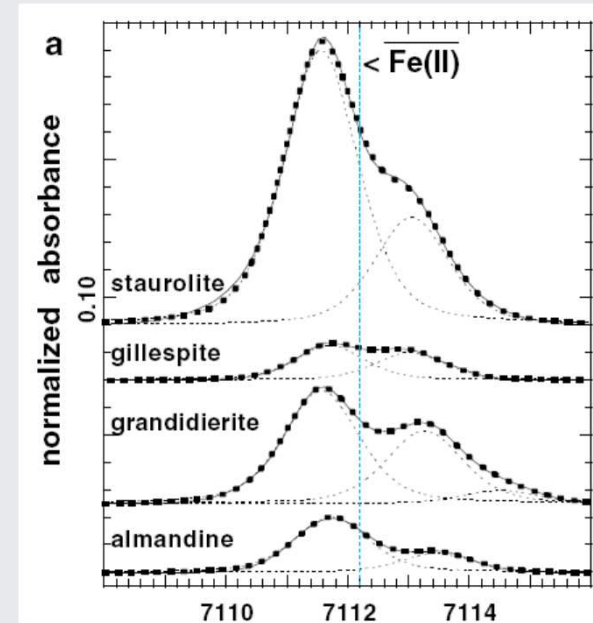
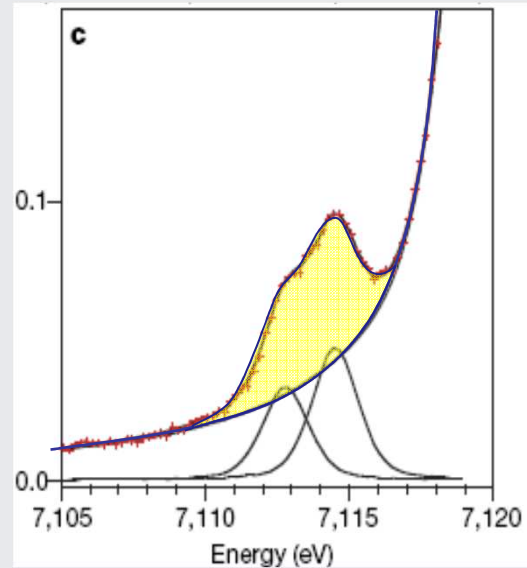
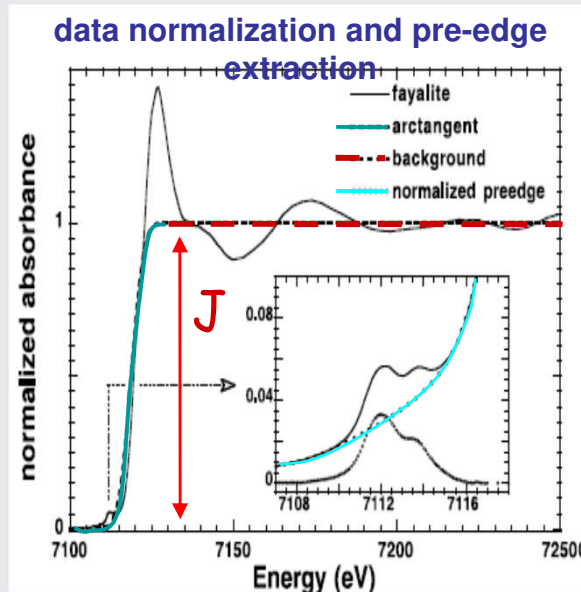


Absorption derivative plot of V K-edge of $\text{PbFe}_{1.75}\text{V}_{4.25}\text{O}_{11}$ sample



V_4O_7

Deconvolution of pre-edge features



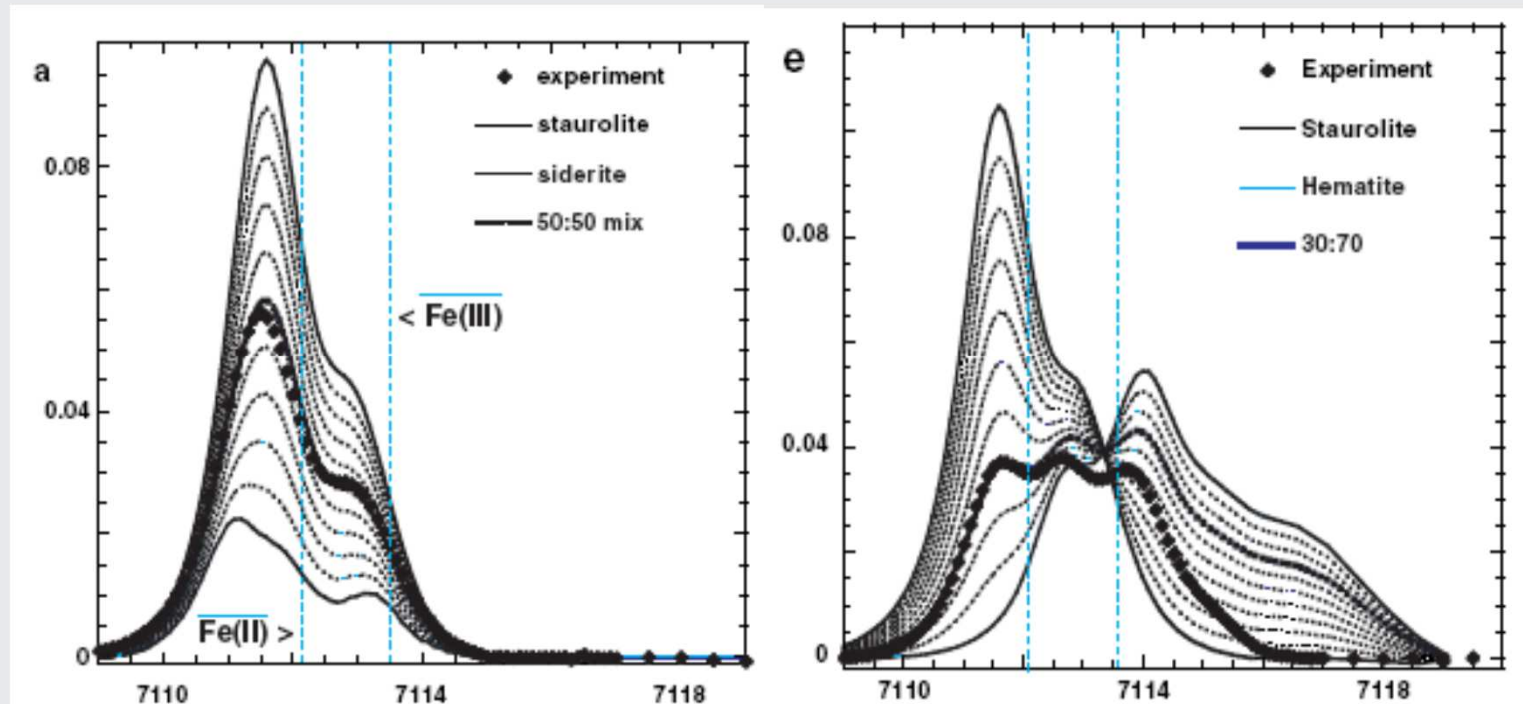
normalization: Jump = 1

arctangent: transitions to continuum states,

peaks: transitions to localized states:

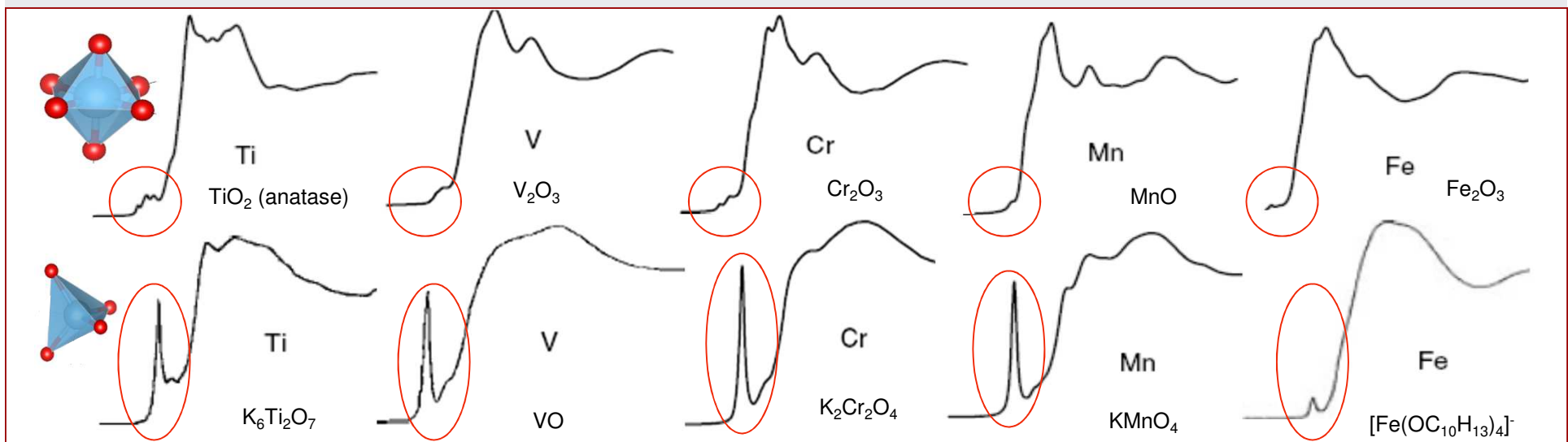
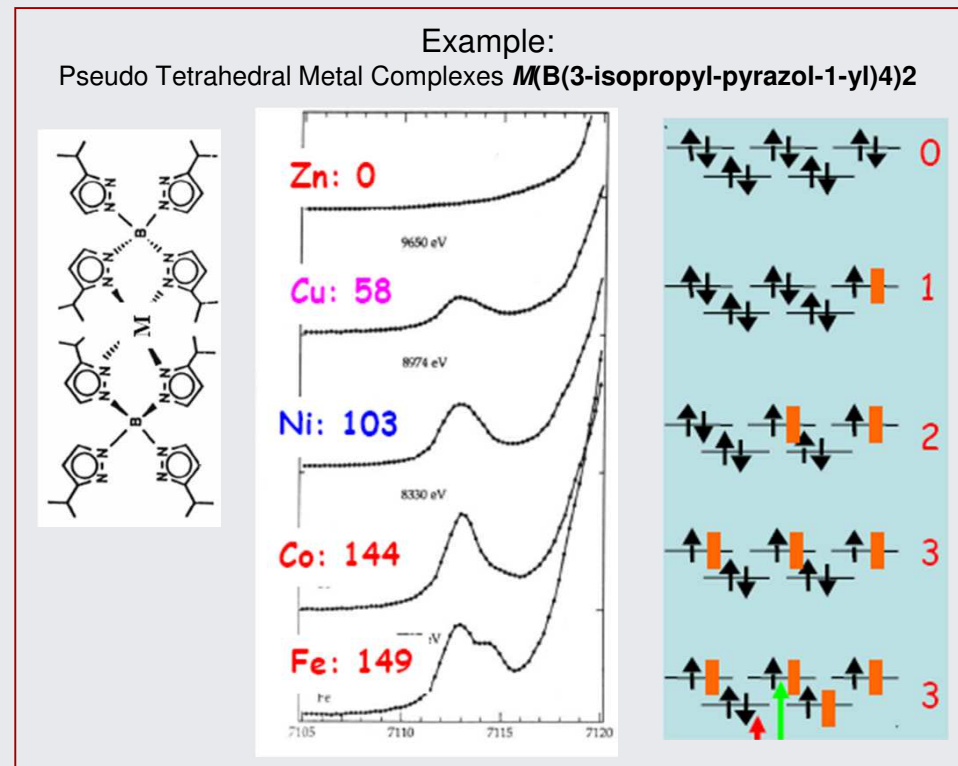
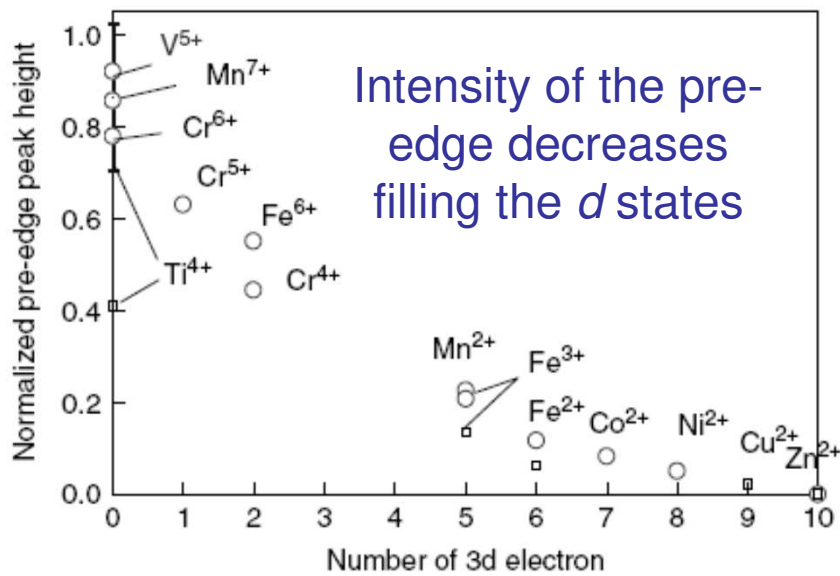
Pseudo-Voigt shaped peaks take into account for the convolution of true peak shape (Lorentzian contribution) with the experimental energy resolution (Gaussian contribution)

linear combination of reference XANES spectra (LCA)



Model compounds data can be used to understand the oxidation states and local coordination environments of the absorber in composite or multiphase materials

K edges of 3d metal oxides... S-d Q-transition?



K edge: mainly $s \rightarrow p$ transitions

$$I_{sd} \text{ (quadrupole)} \sim 10^{-2} I_{sp} \text{ (dipole)}$$

Hybridization mixes p - d states then dipole allowed transitions occur to empty p -components of hybrid pd levels

crystalline field splitting of d atomic orbitals

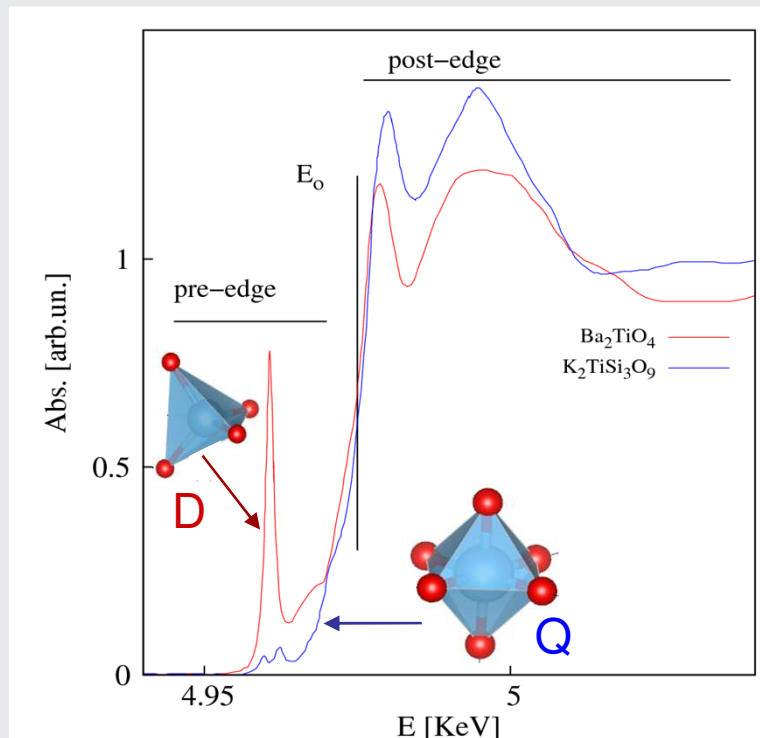
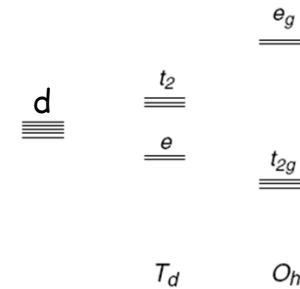


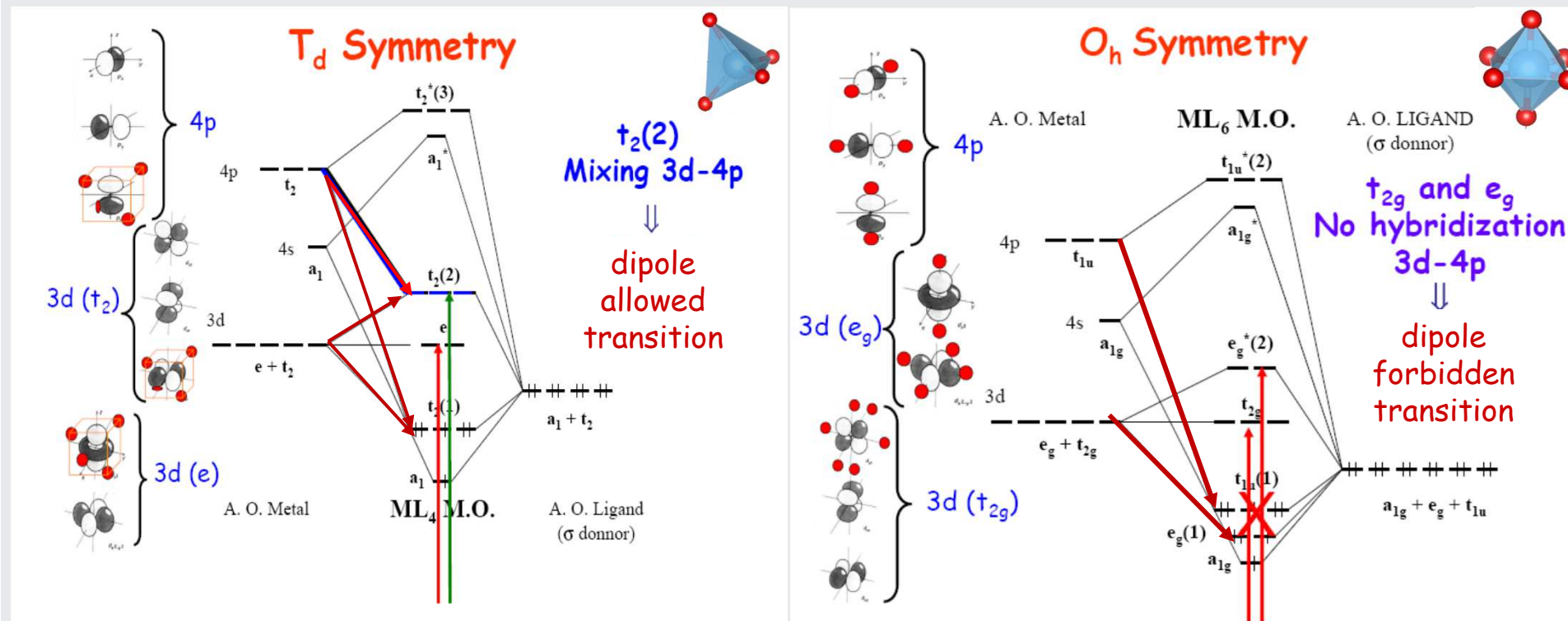
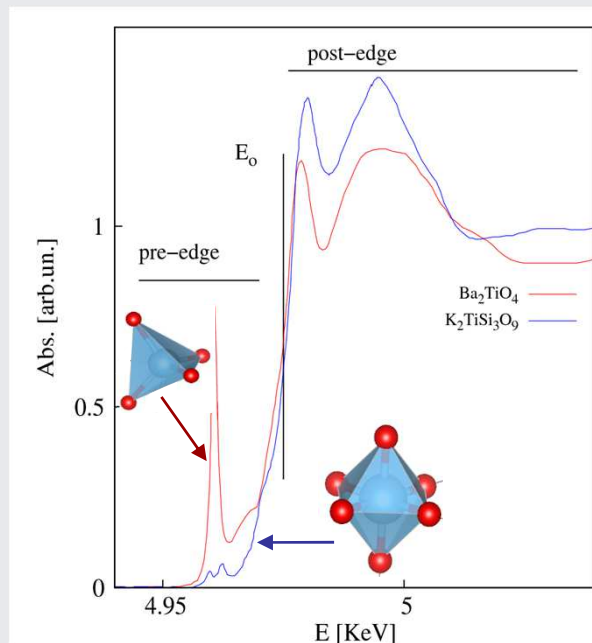
Table 1. Lists of irreducible representations and the relating functions in T_d , O_h , and D_{4h} point groups

T_d		
p	d	
A_1	$x^2 + y^2 + z^2$	
A_2		
E	$(2z^2 - x^2 - y^2, x^2 - y^2)$	
T_1	(R_x, R_y, R_z)	
T_2	(x, y, z)	(xz, yz, xy)
O_h		
p	d	
A_{1g}	$x^2 + y^2 + z^2$	
A_{2g}		
E_g	$(2z^2 - x^2 - y^2, x^2 - y^2)$	
T_{1g}	(R_x, R_y, R_z)	
T_{2g}		(xz, yz, xy)
A_{1u}		
A_{2u}		
E_u		
T_{1u}	(x, y, z)	
T_{2u}		

Yamamoto *X-Ray Spectrom.* 2008; **37**: 572-584

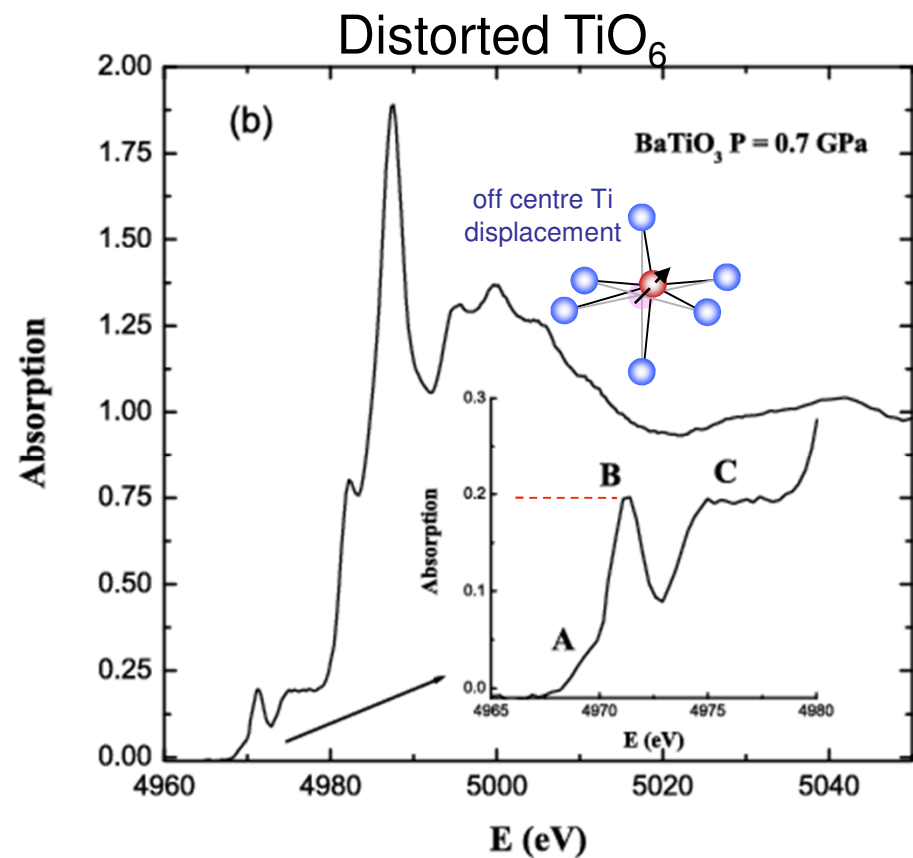
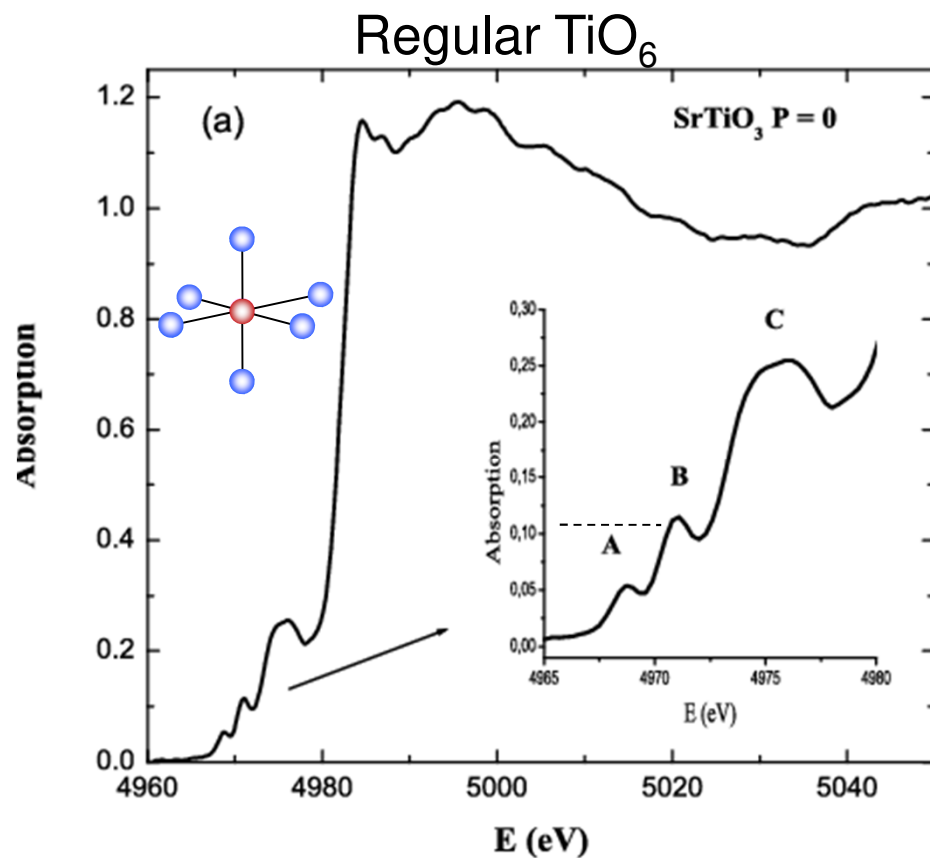
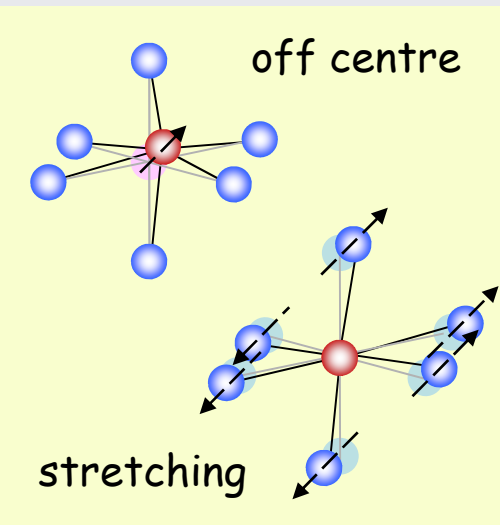
Geometrical origin of pre-edge peaks in Ti oxides

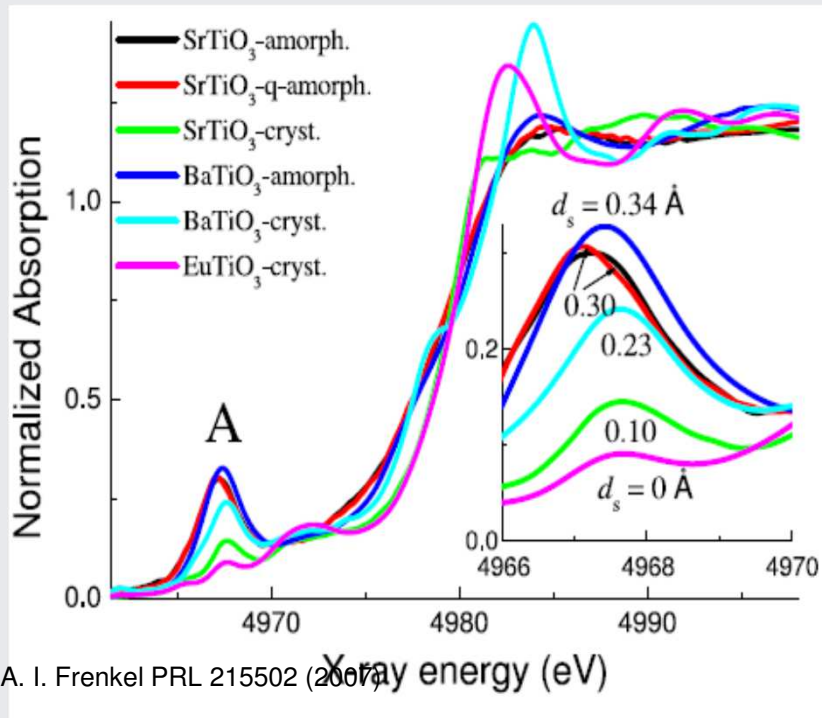
Hybridization mixes p - d states then dipole allowed transitions occur to **empty** p -components of hybrid pd levels



p - d mixing and sensitivity to local symmetry of TiO_6 units

Off centre displacement and stretching of the octahedron decreases the local symmetry (non-centro-symmetric) allowing some degree of p - d mixing, this affect the pre-edge peaks intensity





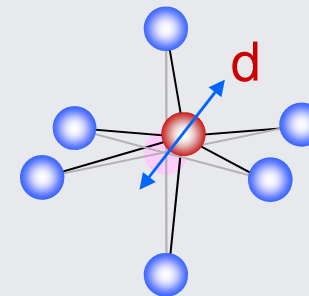
In perovskite structures [1] the area of peak A is proportional to the square of the off center displacement:

$$A = \gamma d^2 / 3$$

for Ti $\gamma = 11.2-13.6 \text{ eV/\AA}$

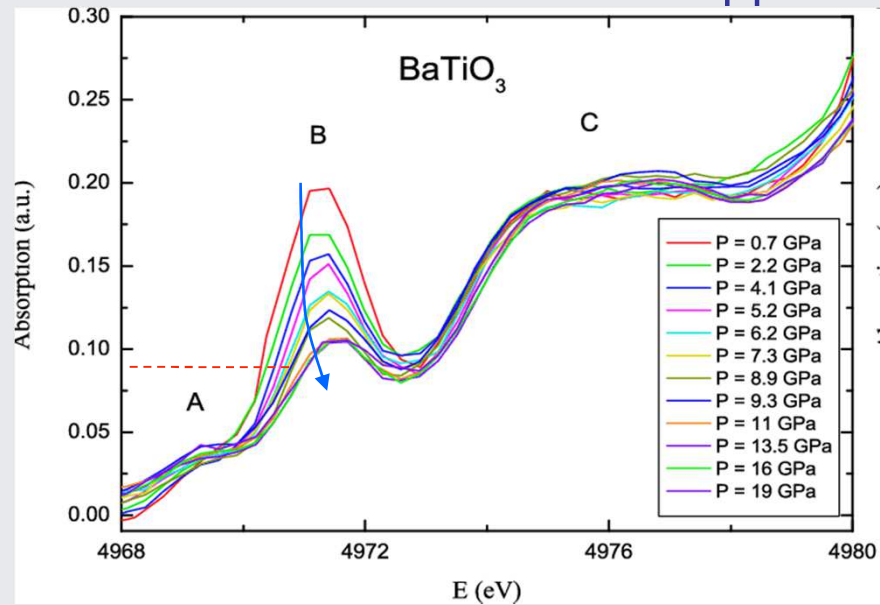
the displacement d contains a static plus a dynamic contribution:

$$d^2 = d_s^2 + d_t^2$$



[1] R.V. Vedrinskii et al. J. Phys. Condens. Matter **10**, 9561 (1998).

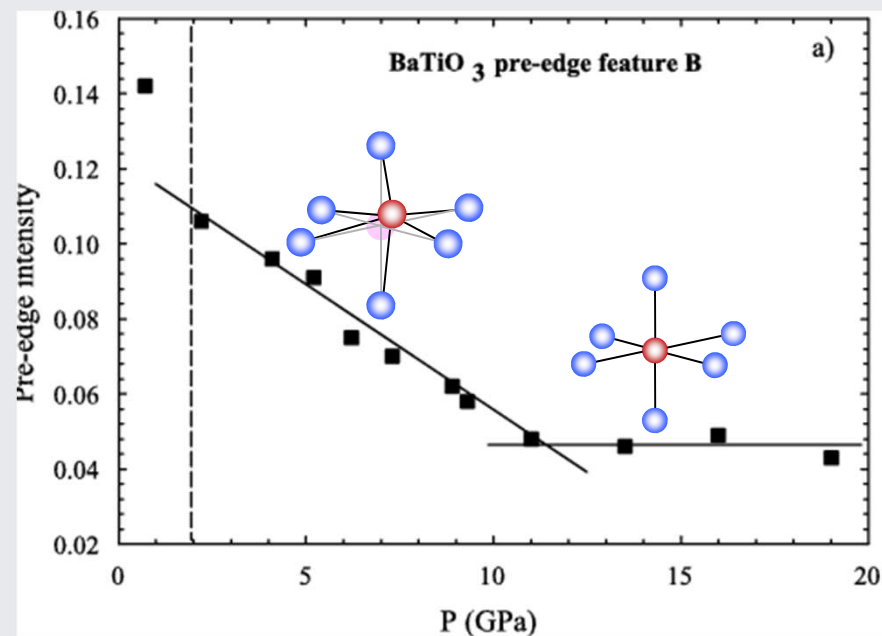
Example: hydrostatic pressure reduces TiO_6 distortions in BaTiO_3 and suppress ferroelectricity



The decrease of B peak intensity signals the reduction of Ti atom displacement.

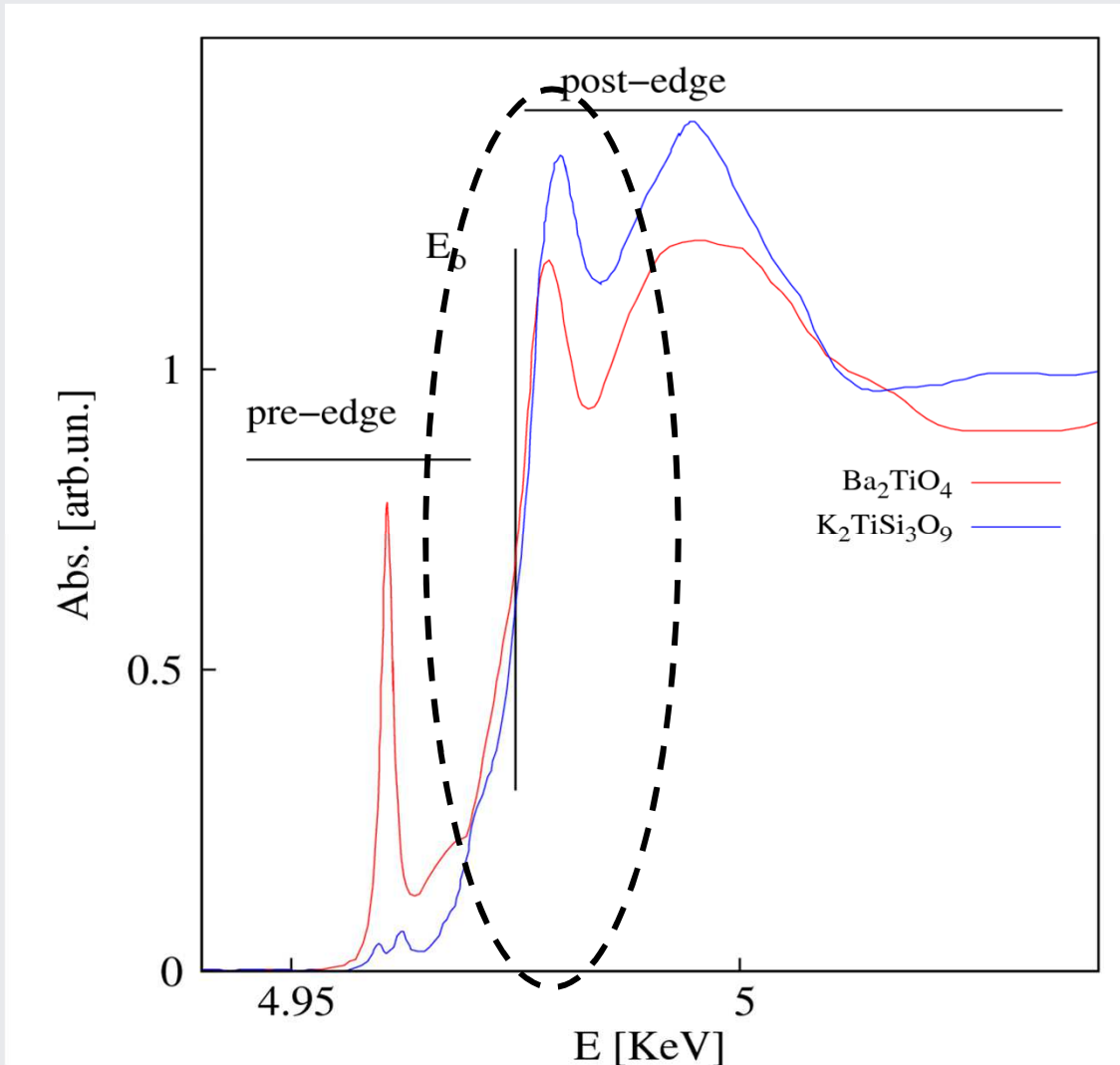
Above 10 GPa Ti must be at the center of a regular oxygen octahedron,

the hybridization of the Ti 3d electronic states with the 2p electronic states of the surrounding oxygen is at the minimum

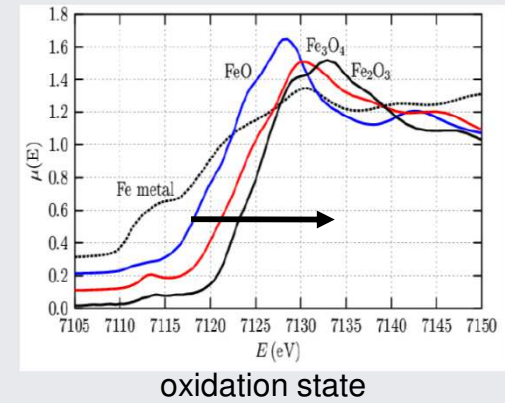


Europhys. Lett., 74 (4), pp. 706–711 (2006)
DOI: 10.1209/epl/i2006-10020-2 J. P. Itié et al.

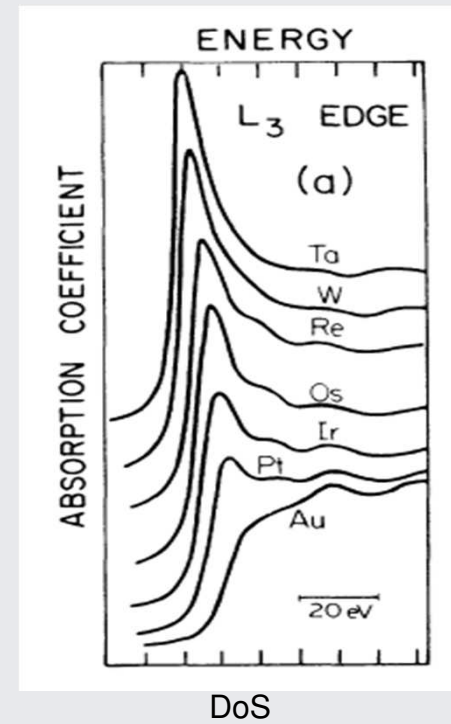
The Edge region



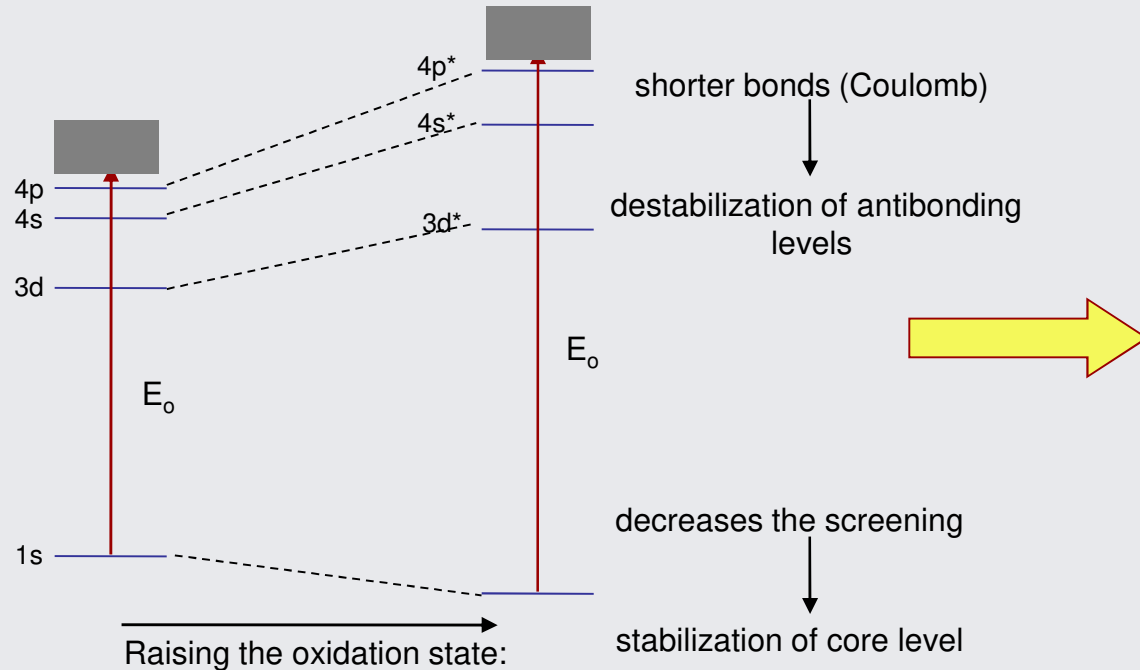
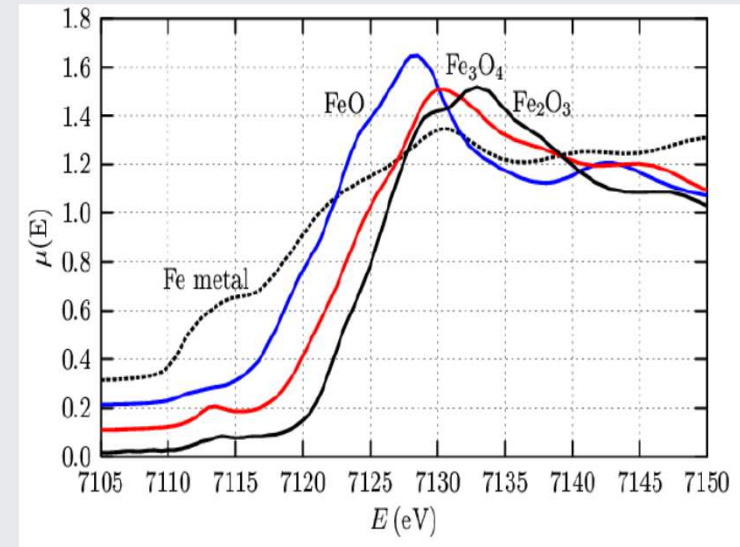
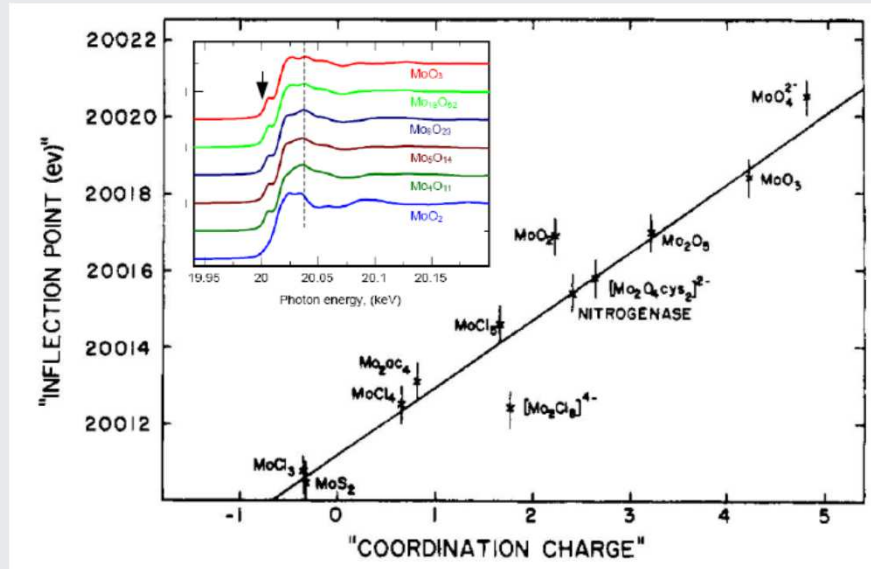
The edge position



The white lines

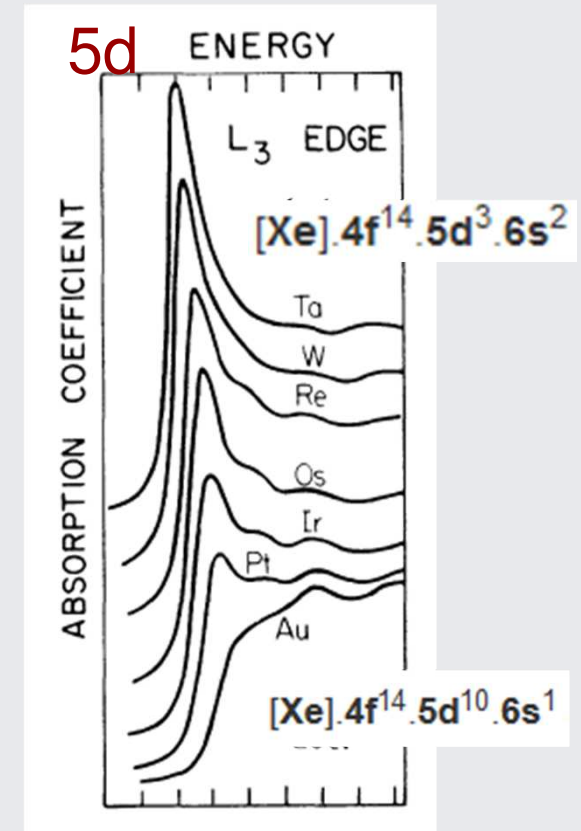
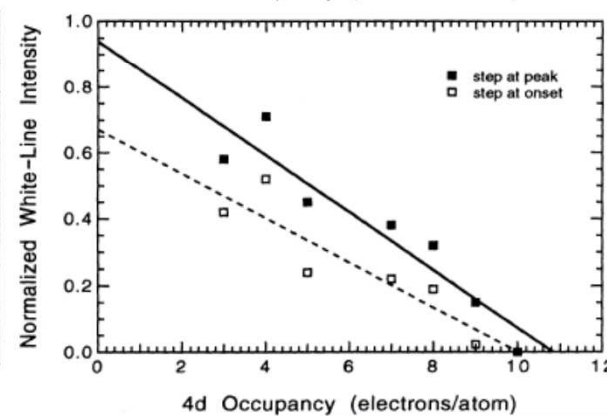
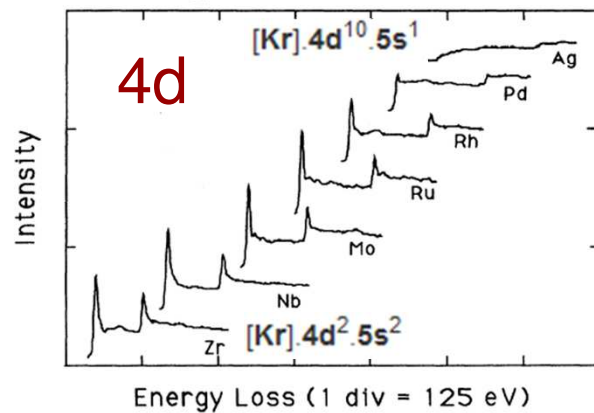
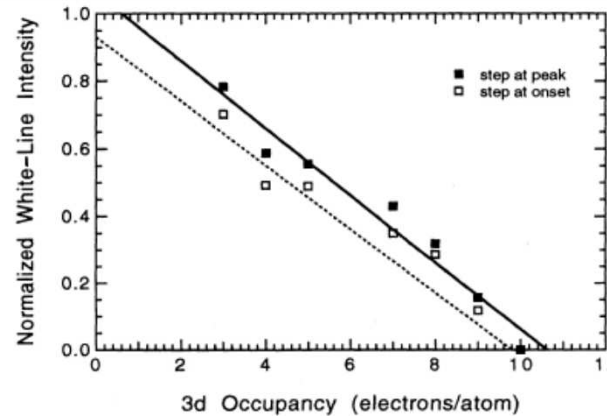
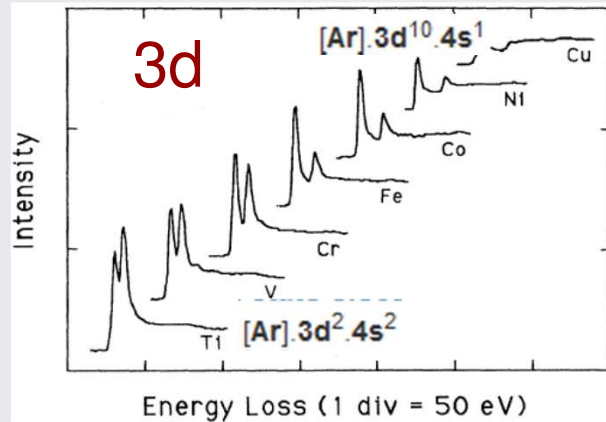


The chemical shift reveals the absorber oxidation state...



**Higher oxidation state
=
High energy shift of the
resonances**

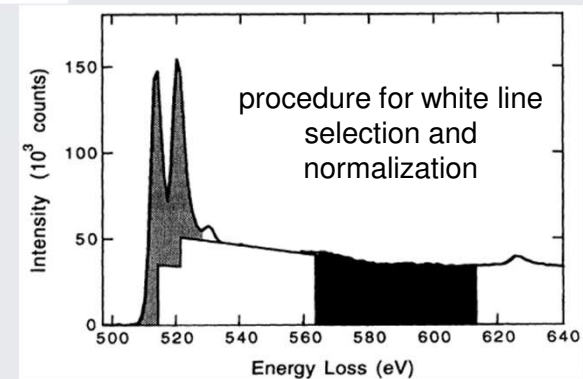
L_{2,3} edge white lines: a probe for occupancy of d band in nd (n=3, 4, 5) elements



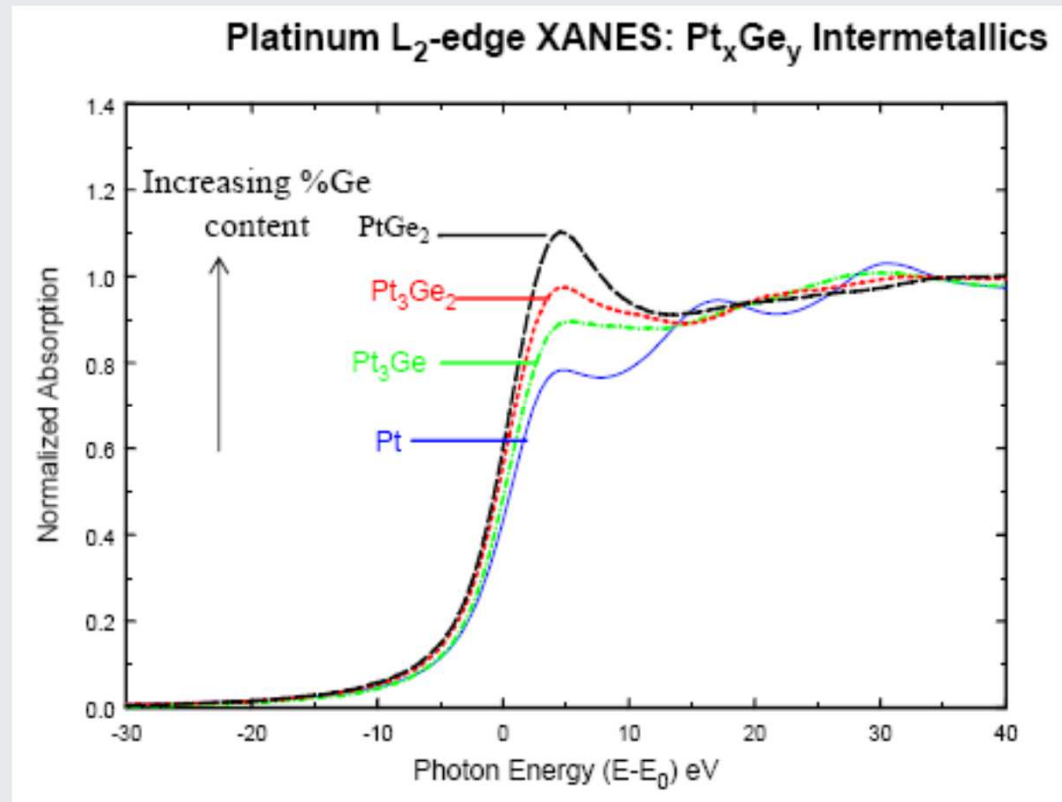
PHYSICAL REVIEW B VOLUME 47, NUMBER 14 1 APRIL 1993-II

White lines and d-electron occupancies for the 3d and 4d transition metals

D. H. Pearson,* C. C. Ahn, and B. Fultz

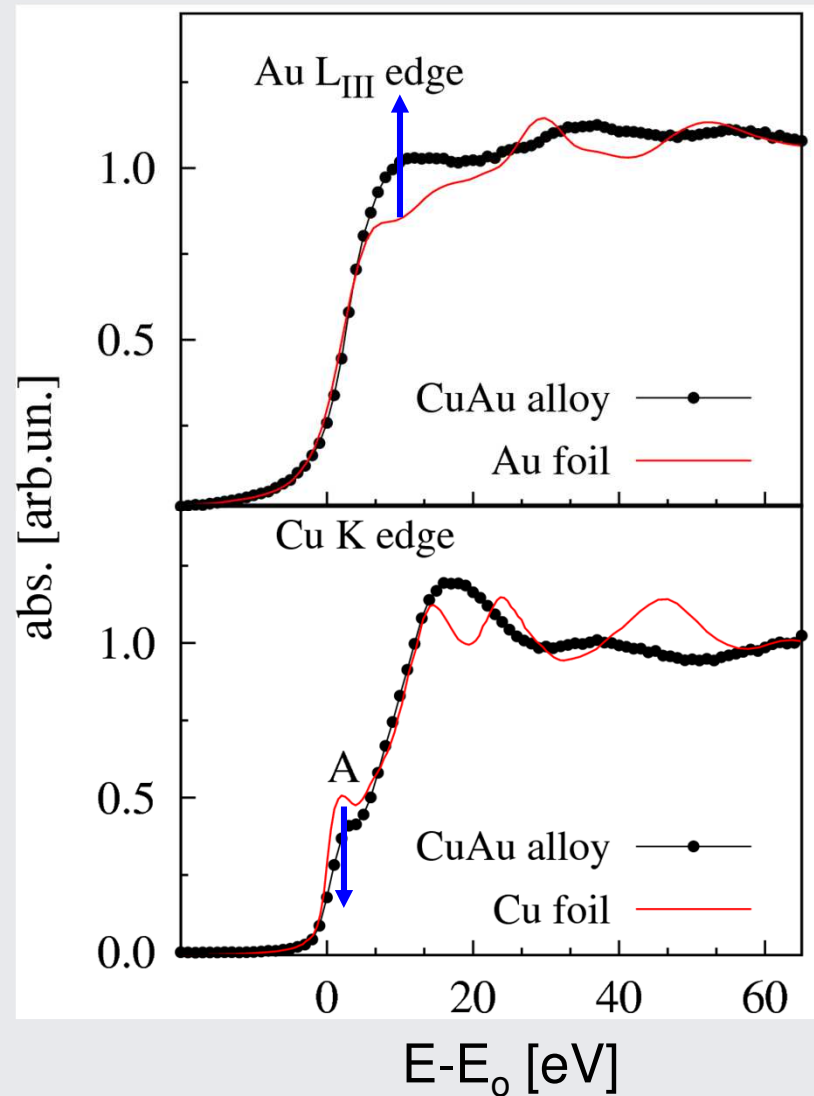


Example: Pt L_2 edge white line in Pt_xGe_y intermetallic compounds



- Transition is $2p$ to $5d$: Pt d -band full, so “no” intensity at edge.
- PtGe intermetallics: charge transfer from d -band of Pt to Ge, resulting in significant intensity at edge.
- Use as signature of Pt-Ge intermetallic formation.

Example: Charge transfer in Cu-Au thin film alloy



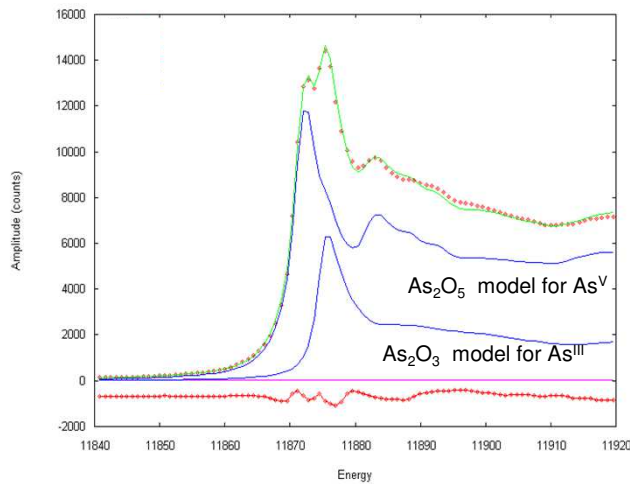
e⁻ migrate from Au
(increasing density of
empty states)
to Cu (decreasing
density of empty
states)

Analysis of mixtures: Linear Combination Analysis

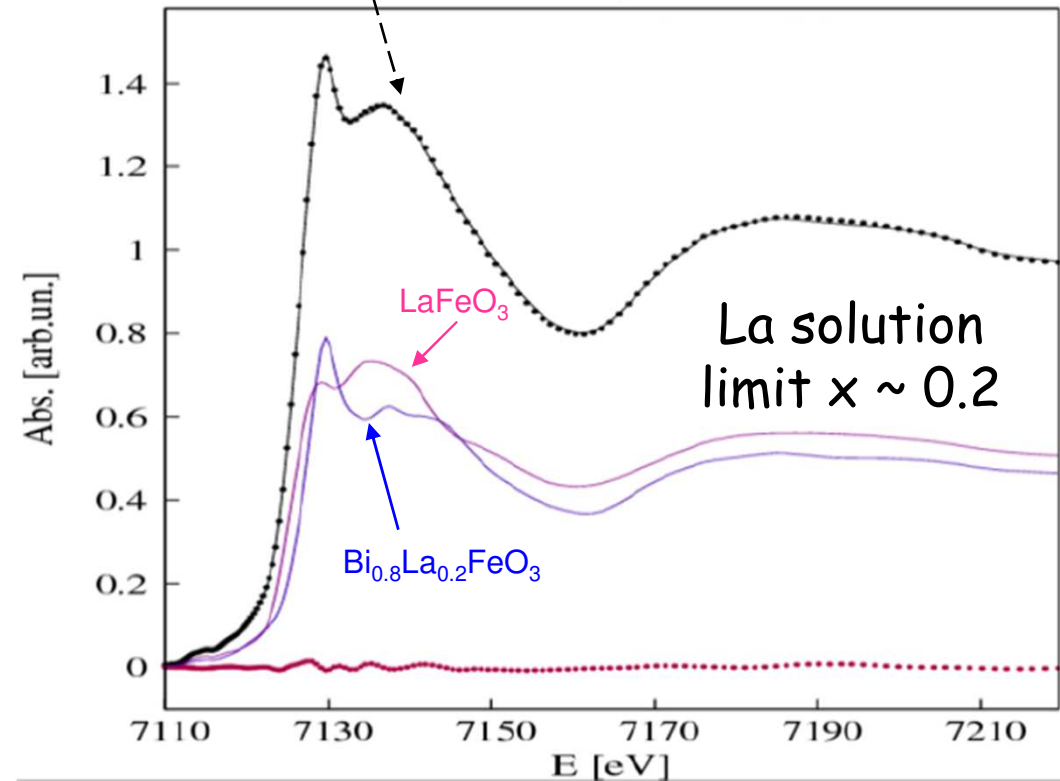
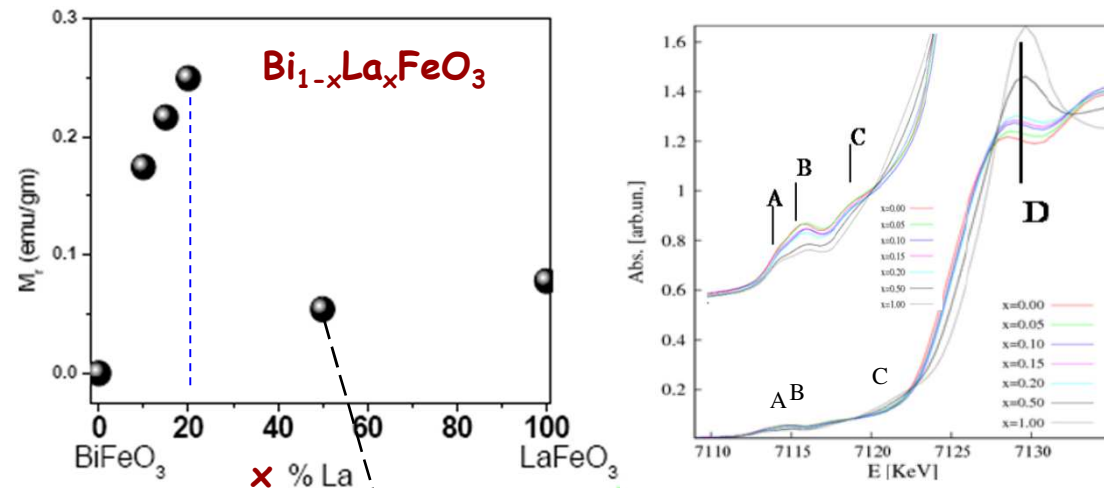
$$\mu^{th} = \sum_j \alpha_j \mu^{ref_j}$$

$$R^2 = \sum_i (\mu^{exp}(E_i) - \mu^{th}(E_i))^2$$

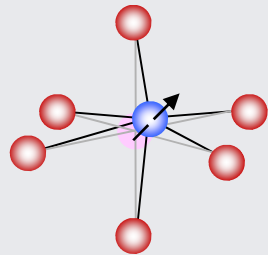
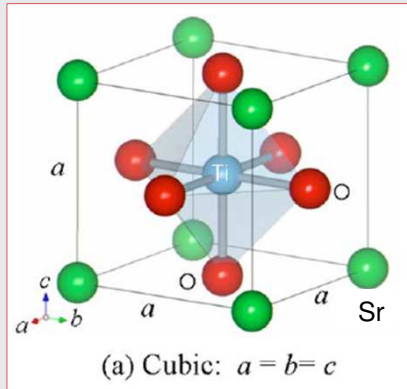
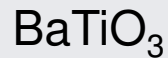
As adsorption in Natural Calcite samples



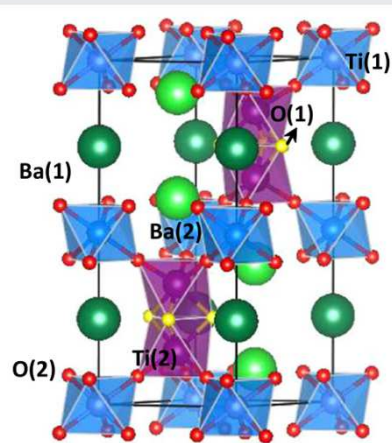
F. Bardelli et al. *Geoch. & cosmochem. acta* 2011



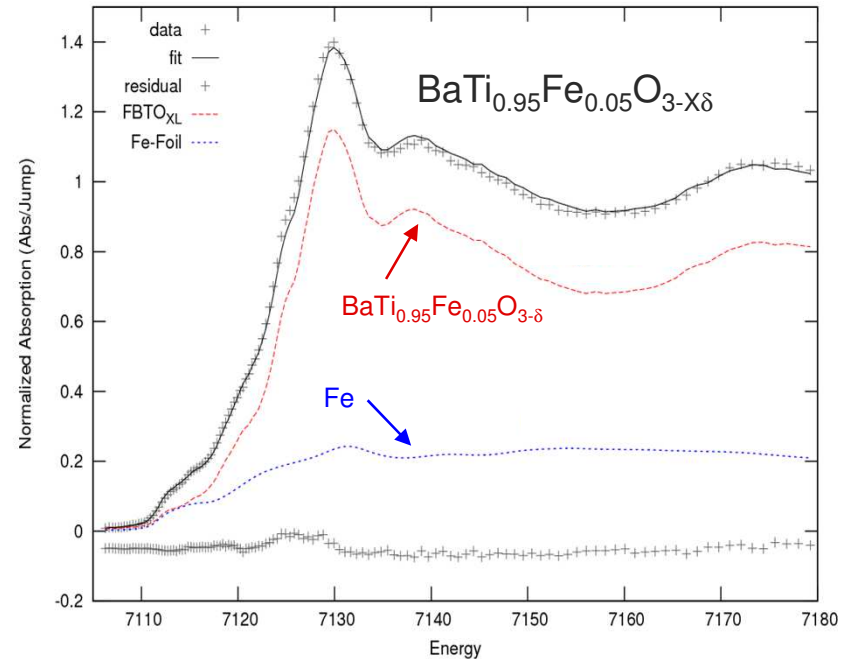
Advanced materials: looking for magneto-electric coupling



BaTiO_3 is **ferroelectric**: off center displacement of Ti^{4+} ions produces a permanent electric dipole in TiO_6 molecules



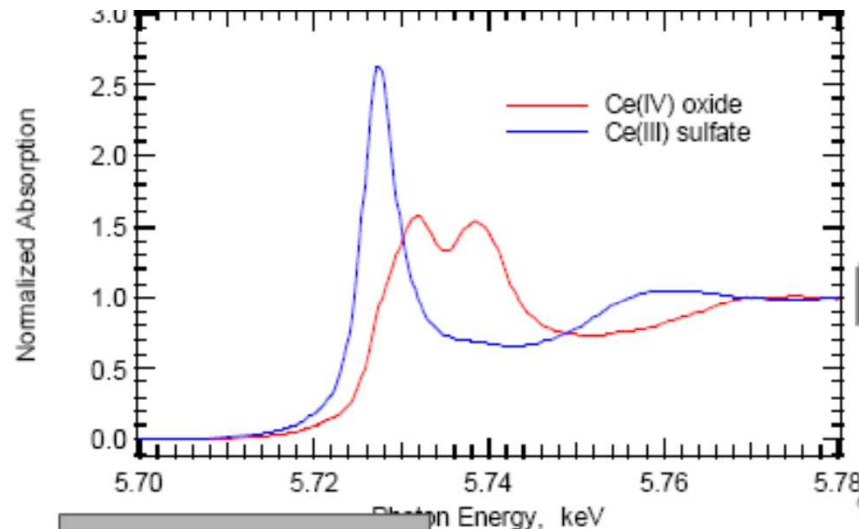
doping with magnetic ions (Fe) may provide some magneto-electric coupling



Large Oxygen vacancies causes the Fe ions segregating as metallic Fe^0 phase, the sample is no more homogeneous at the short range scale, **wrong magneto-electric understanding**

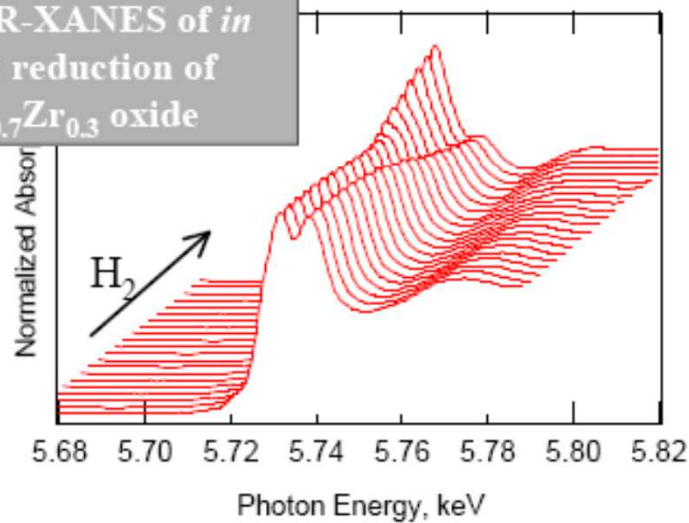
Note: XRD does not show Fe crystalline phase!

LCA-Catalysis

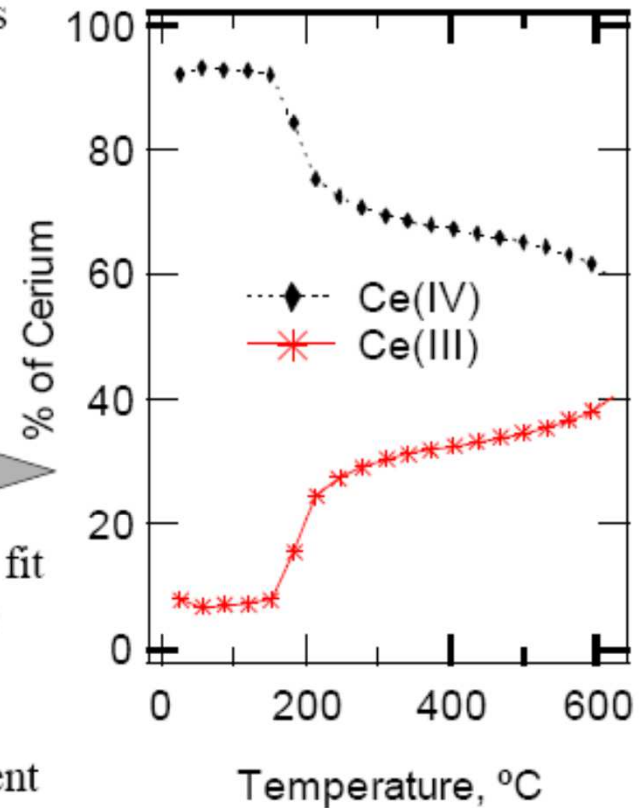


Fit experimental data to linear combination of known reference compounds

TPR-XANES of *in situ* reduction of $\text{Ce}_{0.7}\text{Zr}_{0.3}$ oxide



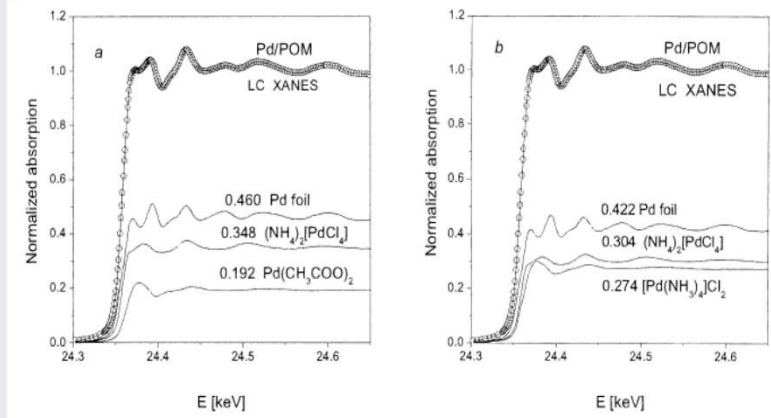
LC-XANES fit to determine amount of Ce(III) and Ce(IV) present as function of temperature



Principal component analysis (PCA)

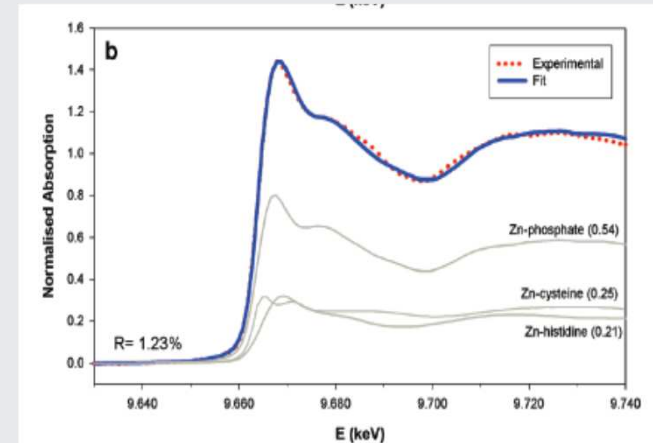
*Determination of molybdenum surface environment of molybdenum/titania catalysts by EXAFS, XANES and PCA. *Mikrochimica Acta* 109 (1992) 281.

PCA, based on linear algebra and statistical methods, is widely used in pattern recognition problems. Each reference spectrum (component) represents a vector, the data are reproduced by vectorial sum. The algorithms automatically determine (statistics) the relevant components (principal) out of a given ensemble and reject the others.



J.W. Sobczak *J. of All. and Comp.* 362 (2004) 162
Local structure of a Pd-doped polymer

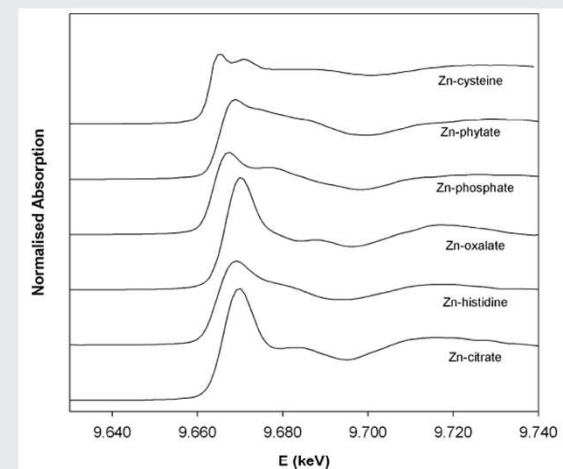
Automatic procedure to select principal components on the basis of their statistical relevance



Warning

- How many standards are necessary?
- Which standards are required?
- Which standards are unphysical?
- Is the final fit reasonable?

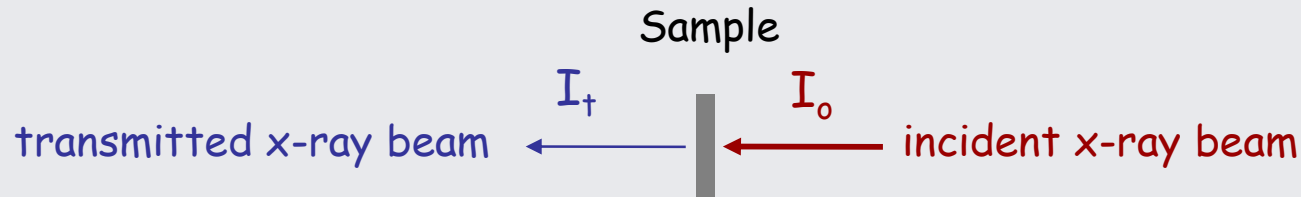
- Use all the a-priori knowledge on the sample (physics, chemistry, etc...)
- Check carefully the results



J. Agric. Food Chem. 2008, 56, 3222-3231

XA(NE)S data collection is conceptually simple

Transmission geometry



$$I_t = I_0 e^{-\mu \cdot x}$$

μ = Linear absorption coefficient

$$\mu x = \ln \frac{I_0}{I_t}$$

Fluorescence geometry

$$I_f \propto I_0 - I_t = I_0(1 - e^{-\mu \cdot x})$$

$$\mu \cdot x \ll 1$$

$$I_f \simeq I_0 \mu \cdot x$$

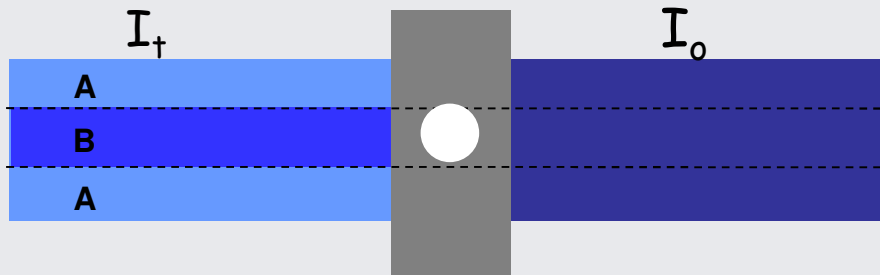
fluorescence intensity



$$\mu x \simeq \frac{I_f}{I_0}$$

... but: some caveat on data collection

Transmission geometry: inhomogeneous samples (i.e. holes) may determine severe distortions of the XA(NE)S spectra

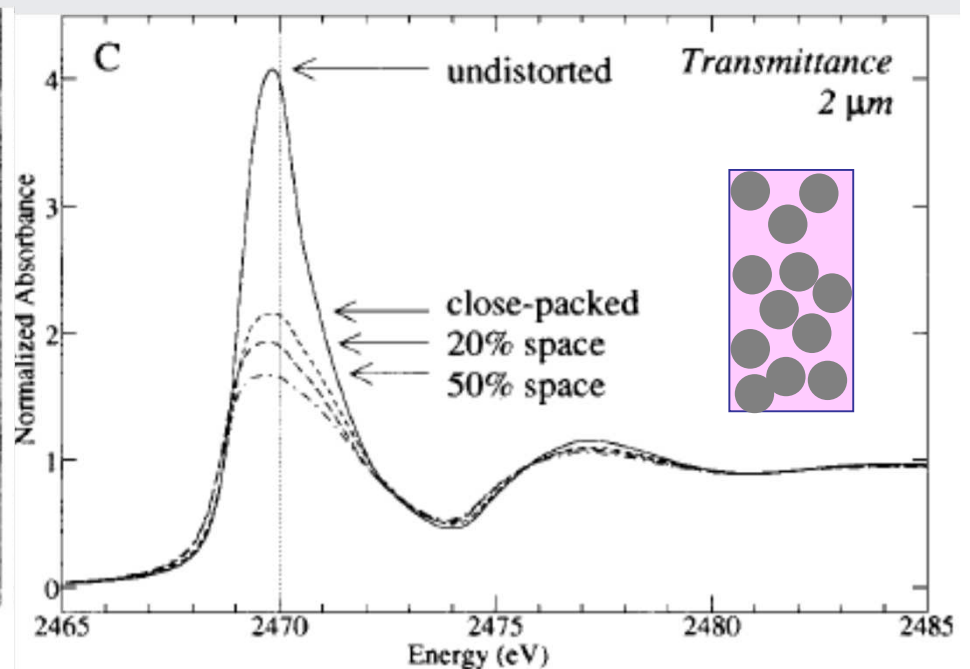
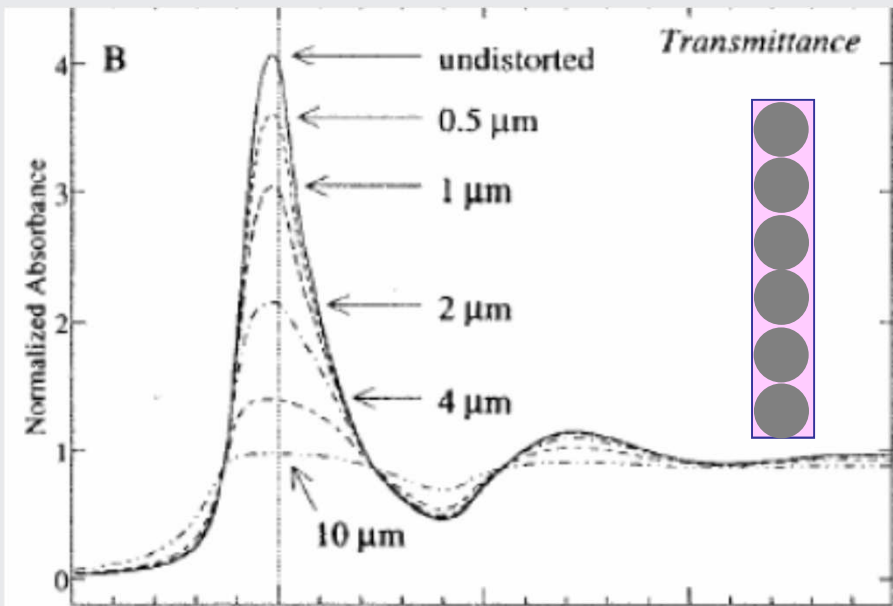


$$I_t = I_o(y_A \cdot e^{-\mu_A x} + y_B \cdot e^{-\mu_B x})$$

$$\ln \frac{I_o}{I_t} = \ln(y_A \cdot e^{-\mu_A x} + y_B \cdot e^{-\mu_B x})$$

S- K edge calculated for a layer of spheres

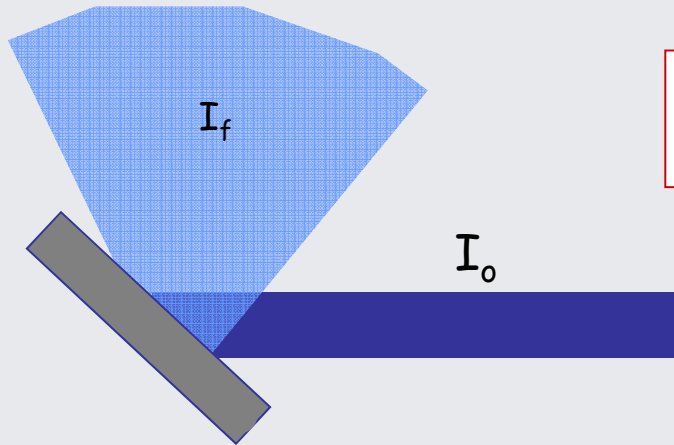
S- K edge calculated for an ensemble of spheres



Pickering et al. Biochem 40 92001) 8138

some caveat on data collection

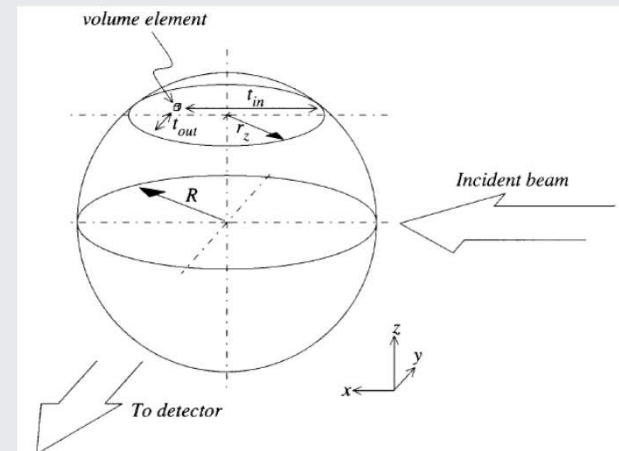
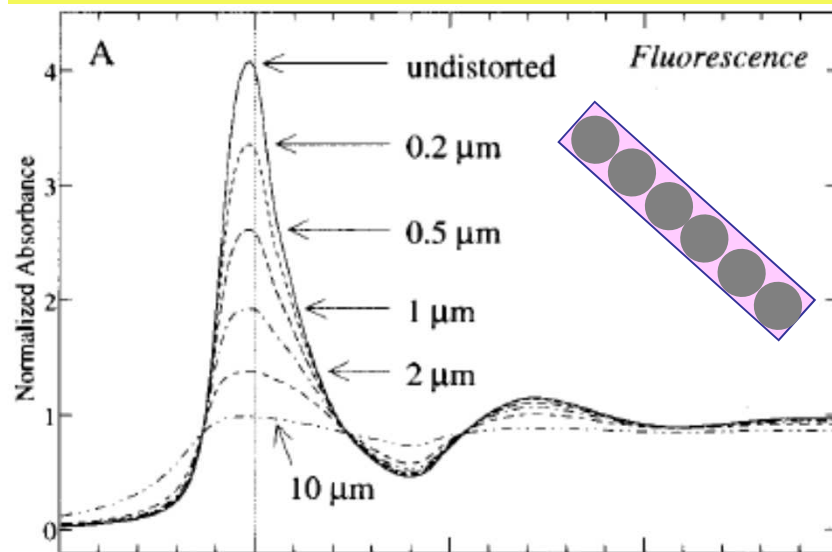
Fluorescence geometry: re-absorption and detector linearity may determine severe distortions of the XA(NE)S spectra



$$I_f \propto I_0 - I_t = I_0(1 - e^{-\mu x}) \simeq I_0 \mu x$$

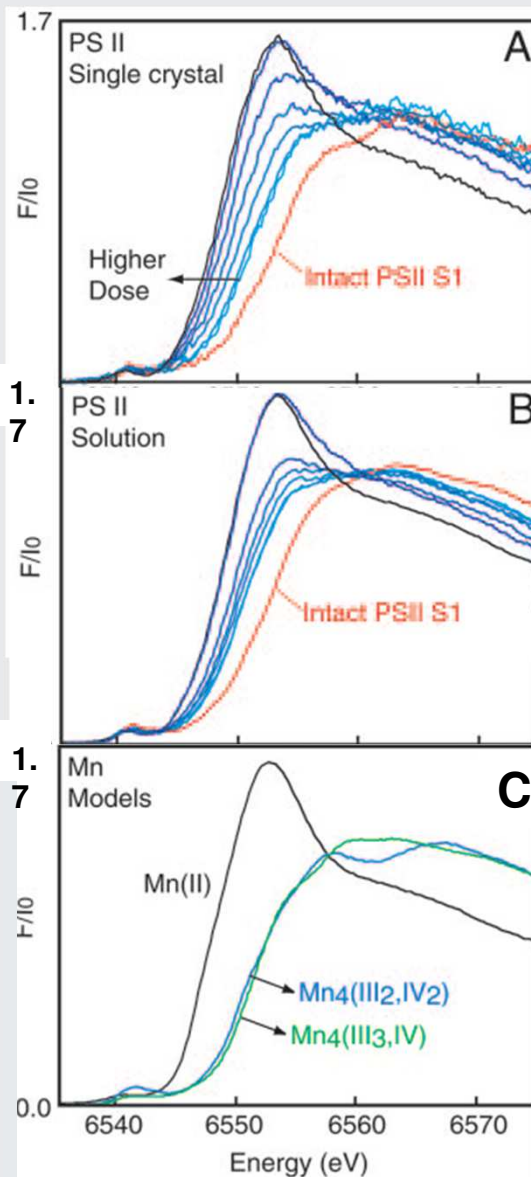
$$\mu x \ll 1$$

effect of particle size (spheres) on I_f



some caveat on data collection

photoreduction on
 Mn_4Ca PS(II) complex



Proc. Natl. Acad. Sci. USA 102, 12047 (2005)

Radiation Damage & photoreduction

R.D. is a function of exposure time/dose, provoke shift of the edge and deformation of XAFS features.

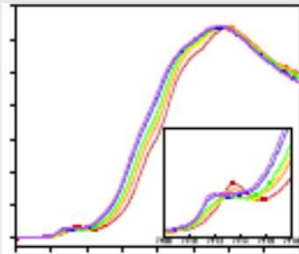
R.D. can be reduced by:

- reducing the x-ray intensity
- reducing the exposure time
- collecting data at low sample temperature

R.D. can be very relevant in biological samples like metalloproteins.

Details about radiation damage and photoreduction can be relevant for reliable
protein crystallography

Radiation Damage: XAS and Crystallography



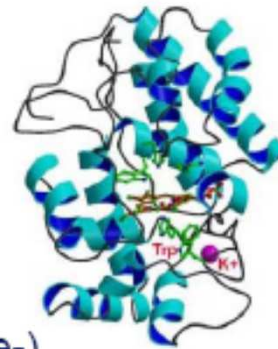
XAS

Visible Effect

- Edge shift (~ 1 eV per e-)
- Shift in EXAFS peak positions

Structural Effect

- *Can be monitored over time (repeated single scans)*
- Longer Metal-Ligand bonds and/or increased σ^2 in M-L paths
- Change in site geometry due to irradiation/chemical reaction



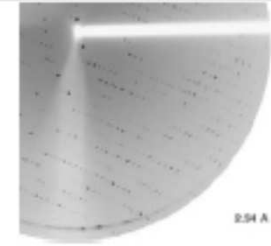
PX

Visible Effect

- Loss of diffraction intensity
- Increased unit cell volume

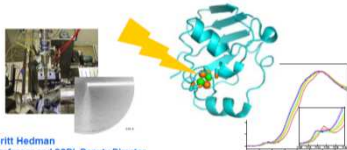
Structural Effect

- *Not monitored over time (one cumulative data set)*
- Breakage of selected bonds
 - High DW-factors
- Loss of or unexplained density



Fifth International Workshop on X-ray
Damage to Biological Crystalline Samples
Paul Scherrer Institut, Villigen, March 3-6, 2008

Photoreduction of Metalloprotein Active Sites by
Synchrotron Radiation

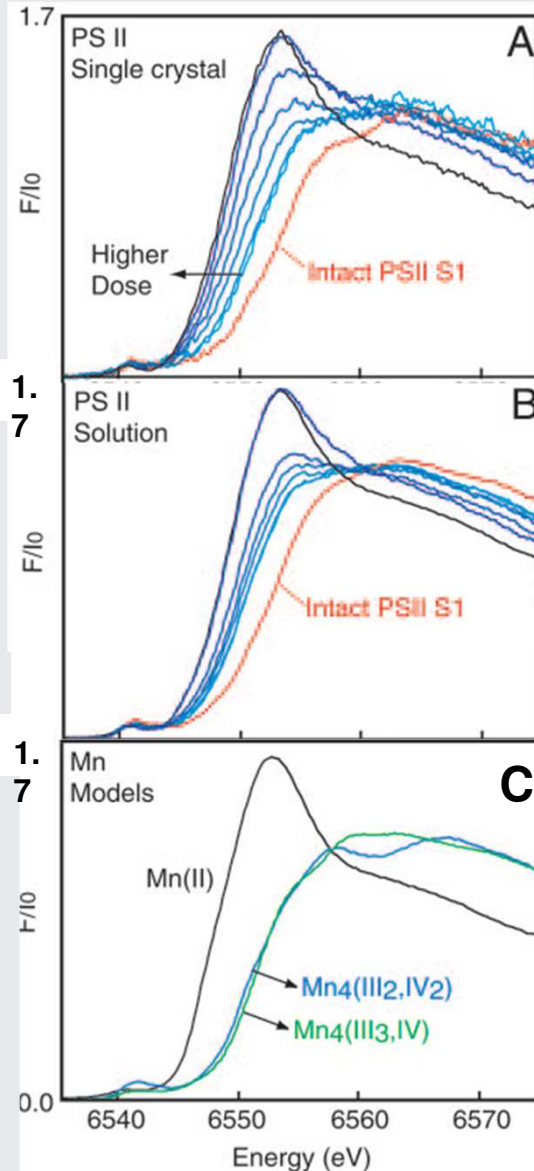


Britt Hedman
Professor and SSRL Deputy Director
The SSRL program is funded by DOE-BER, NIH-NCRR, NIH-NIGMS, PRT and Collaborative Partners

XAFS can be used to monitor (in situ)
photoreduction of metals

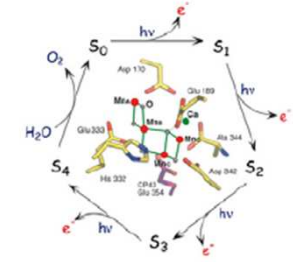
X-ray damage to the Mn₄Ca complex in single crystals of photosystem II: A case study for metalloprotein crystallography

Junko Yano^{1,2}, Jan Kern^{3,5}, Klaus-Dieter Irrgang², Matthew J. Latimer³, Uwe Bergmann³, Pieter Glatzel¹, Yulia Pushkar¹, Jacek Biesiadka^{1,2}, Bernhard Loll^{1,2}, Kenneth Sauer¹, Johannes Messinger^{1,2,3}, Athina Zouni^{1,2}, and Vittal K. Yachandra^{1,2}



Proc. Natl. Acad. Sci. USA 102, 12047 (2005)

Photosynthesis uses light energy to produce O₂ and fix CO₂. This process generates an aerobic atmosphere and produces a readily usable carbon source.



Photosystem II (PSII) reaction catalyzes the photoinduced oxidation of water so it plays an essential role in maintaining the biosphere

It is of considerable importance to elucidate its catalytic mechanisms, particularly those involved in the water oxidation process.

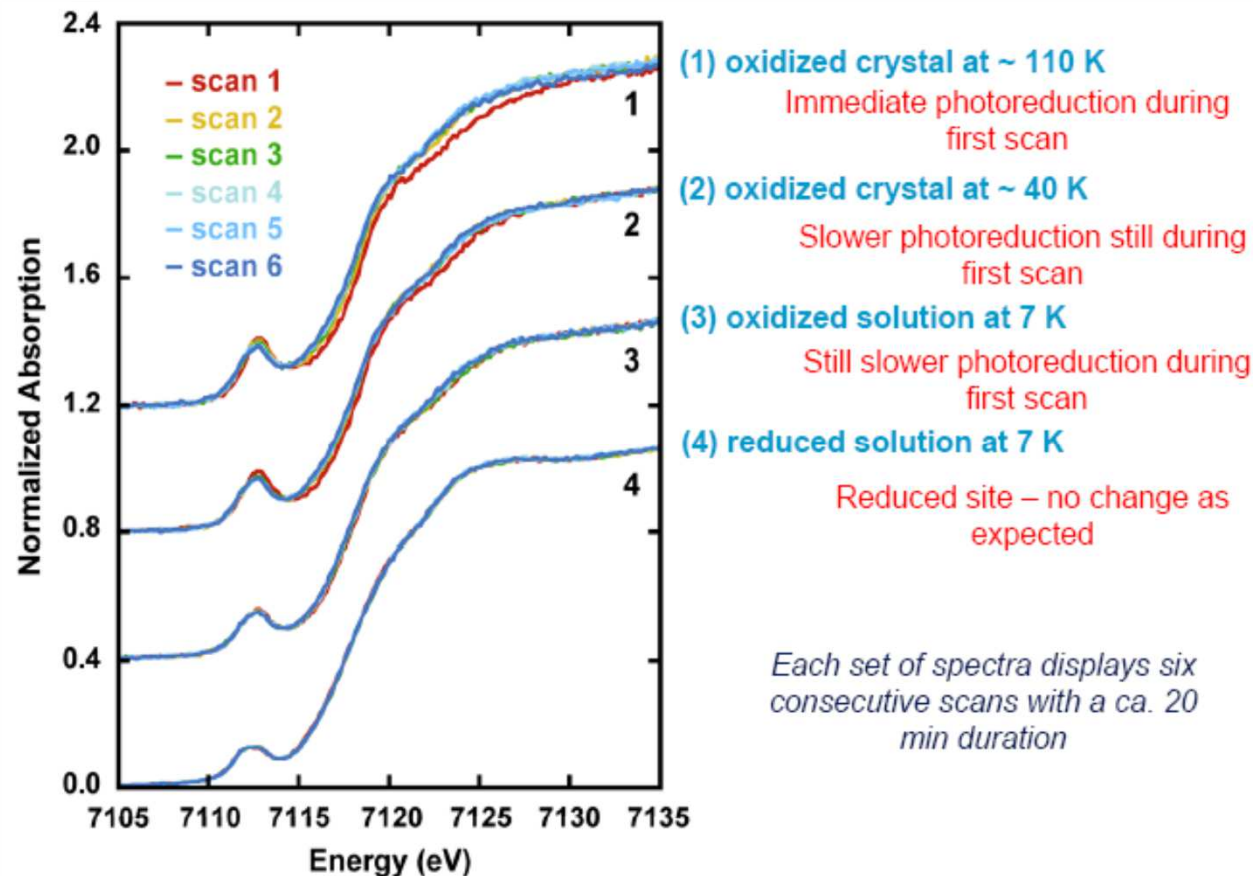
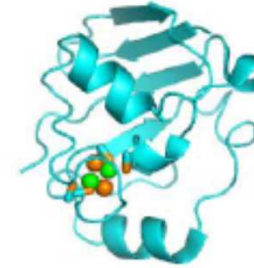
...at present, there are **serious discrepancies** among the models of the structure of the Mn₄Ca complex in the published **x-ray crystallography** studies, and there are inconsistencies with **x-ray, EPR, and FTIR** (...). **This disagreement is predominantly a function of x-ray-induced damage to the catalytic metal site** (...) Therefore, the reported **model of the Mn₄Ca complex** at atomic detail **cannot be based on the diffraction data only** (...).

Proc. Natl. Acad. Sci. USA 102, 12047 (2005)

photo-reduction of Mn ions

Radiation Damage and photoreduction

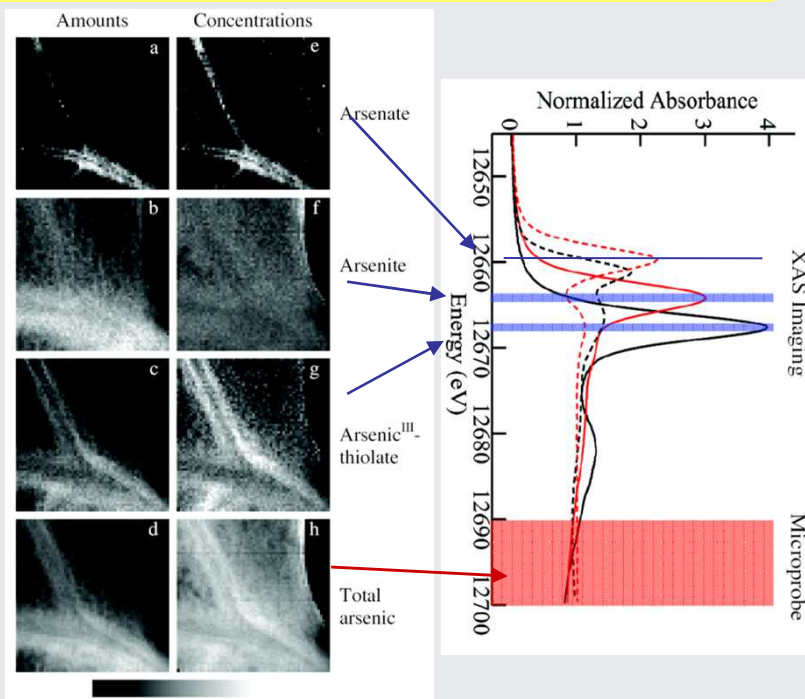
The PDB lists 40 structures for $[\text{Fe}_2\text{S}_2]\text{Cys}_4$ ferredoxins
8 are described as oxidized, 1 is described as reduced
none include spectroscopy that would verify the redox state!



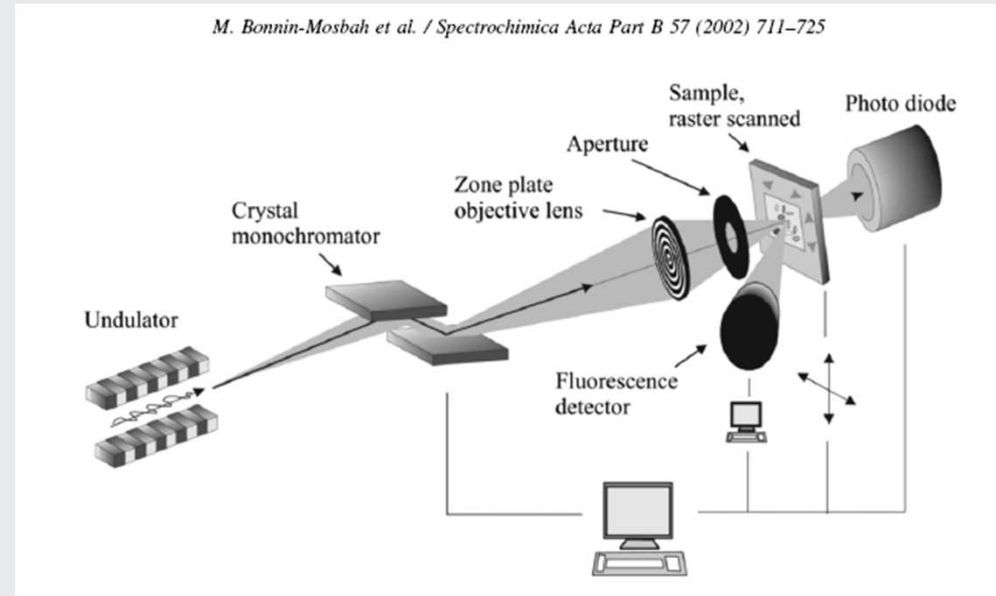
Other applications of XANES spectroscopy: μ -XANES & mapping

Notice:

μ (n)-XRF= elemental sensitivity
 μ (n)-XAS= **elemental sensitivity + chemical speciation**



I. J. Pickering & G. N. George Proc. XAFS13 conference (2006)



M. Bonnin-Mosbah et al. / Spectrochimica Acta Part B 57 (2002) 711-725

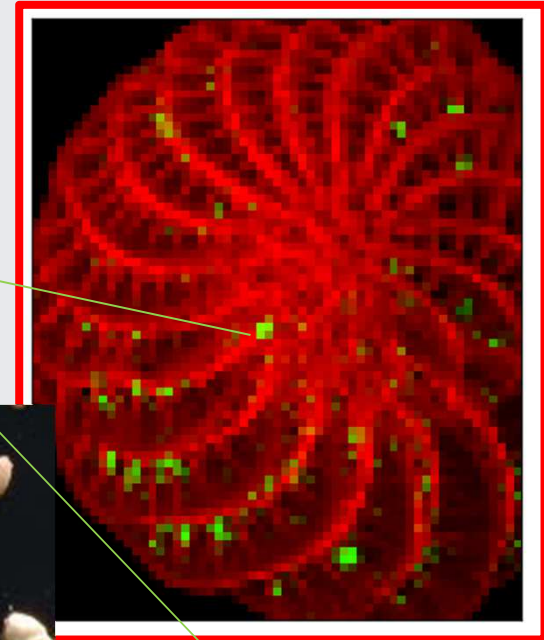
X-ray lenses and zone plates work in a reduced energy window, therefore the EXAFS region is often not accessible to micro and nano probes

Bio- e Fito-Remediation or:
Plants and (micro-)organisms employed to regulate pollutant mobility (i.e. heavy metals) within the ecosystem and environment

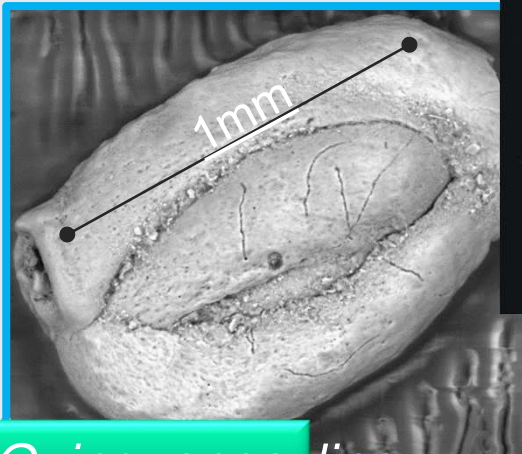
Elphidium



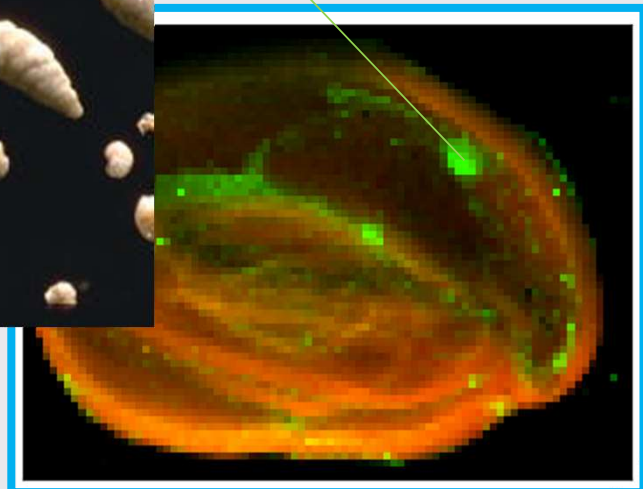
μ -XANES & mapping



Foraminiferi

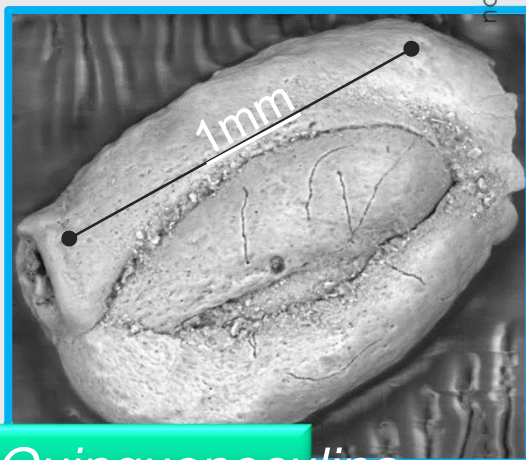


Quinquenoculina



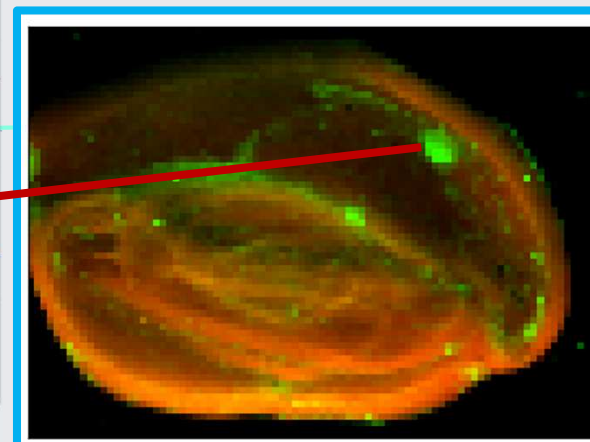
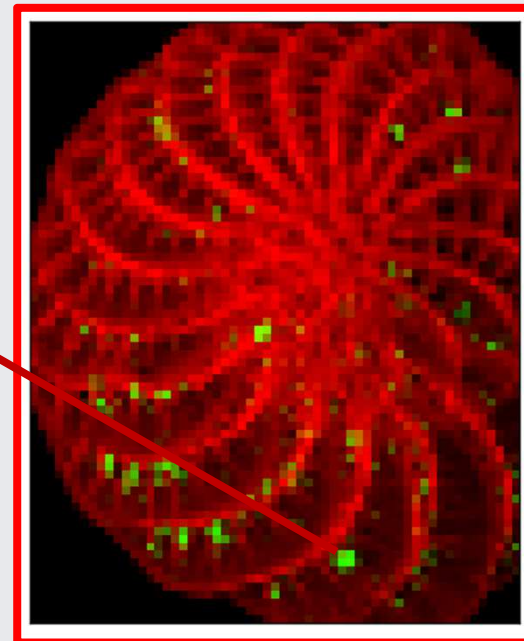
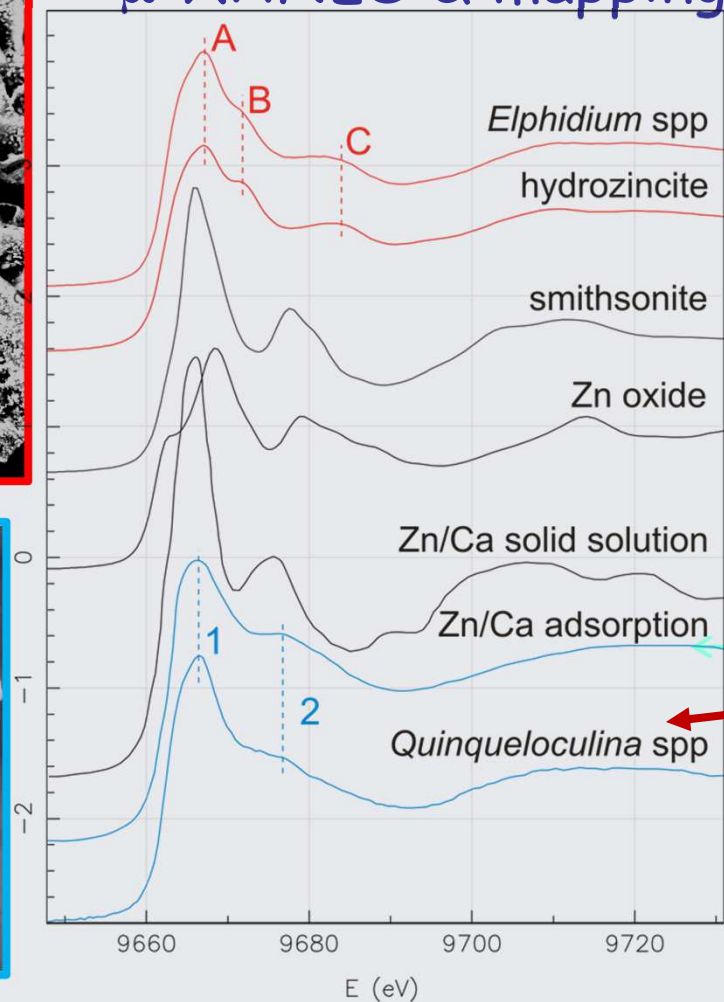
Bio- e Fito-Remediation or:
Plants and (micro-)organisms employed to regulate pollutant mobility (i.e. heavy metals) within the ecosystem and environment

Elphidium



Quinquenoculina

μ -XANES & mapping



Time resolved XA(NE)S: experimental set-up

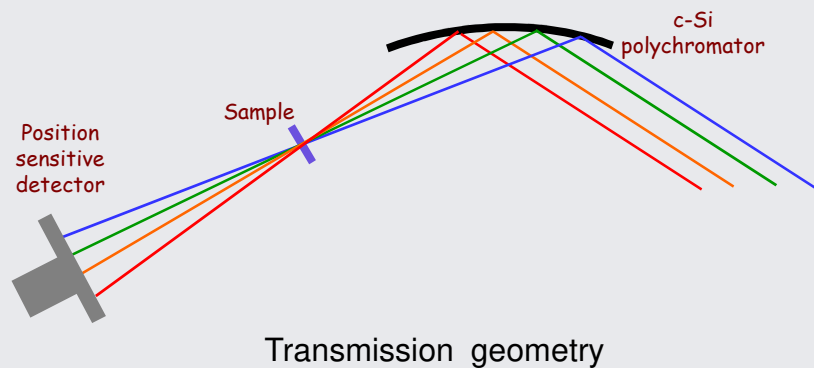
Quick XAFS

$$\Delta t = 10^{-10} - 10^{-2} \text{ s}$$

any data collection geometry

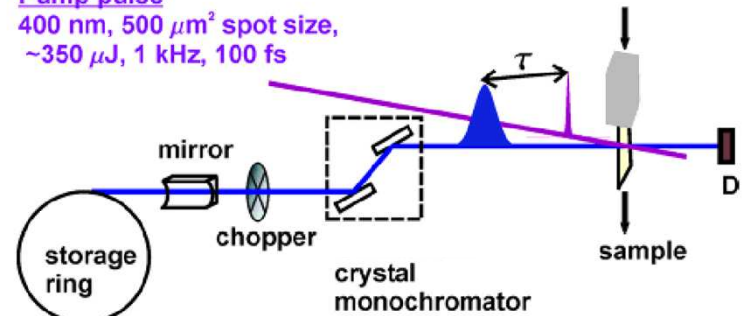
Dispersive XAFS

$$\Delta t = 10^{-3} - 1 \text{ s}$$



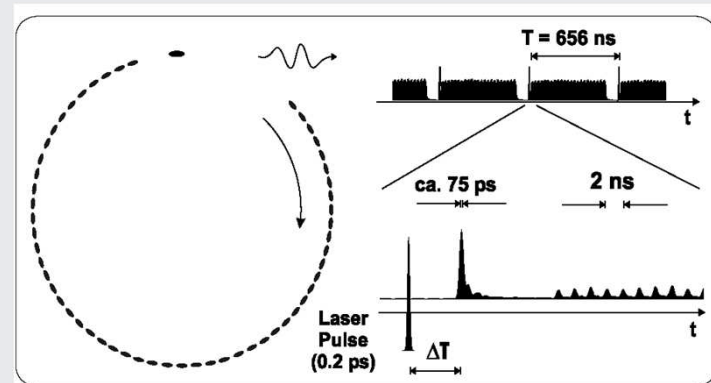
Pump probe

Pump pulse
400 nm, 500 μm^2 spot size,
 $\sim 350 \mu\text{J}$, 1 kHz, 100 fs



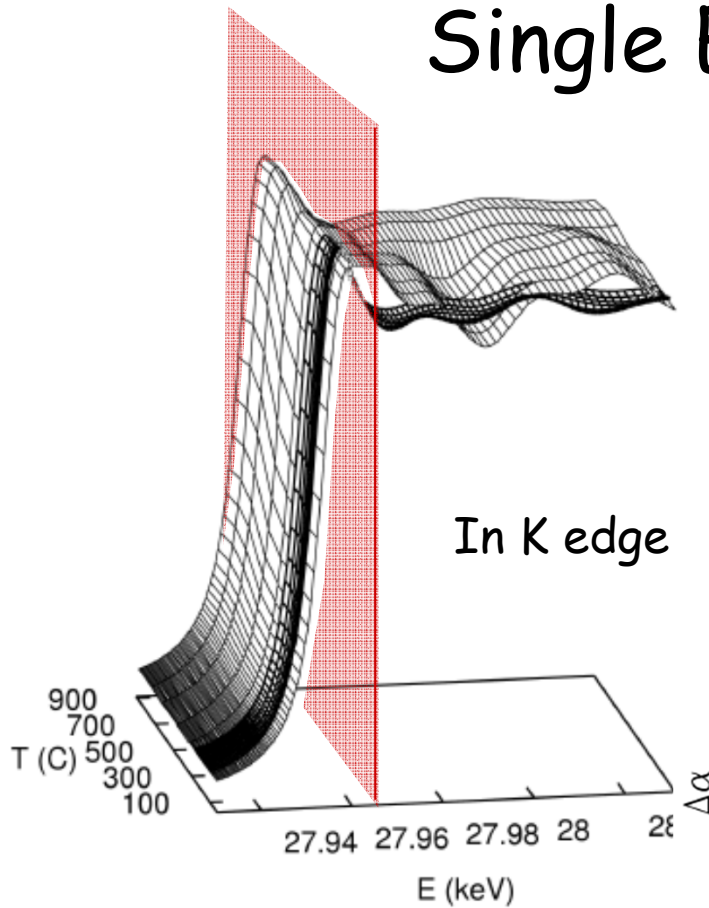
X-ray probe
7.1 keV, 300 μm^2 spot size, 70 ps
500-1000 photons/pulse/0.1% bandwidth

$$\Delta t < \text{ns}$$

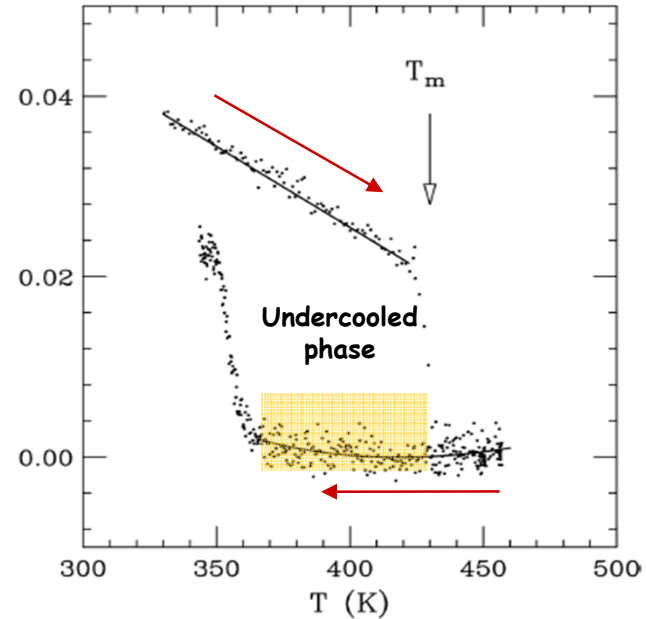


Time resolved XAS

Single Energy - XAS

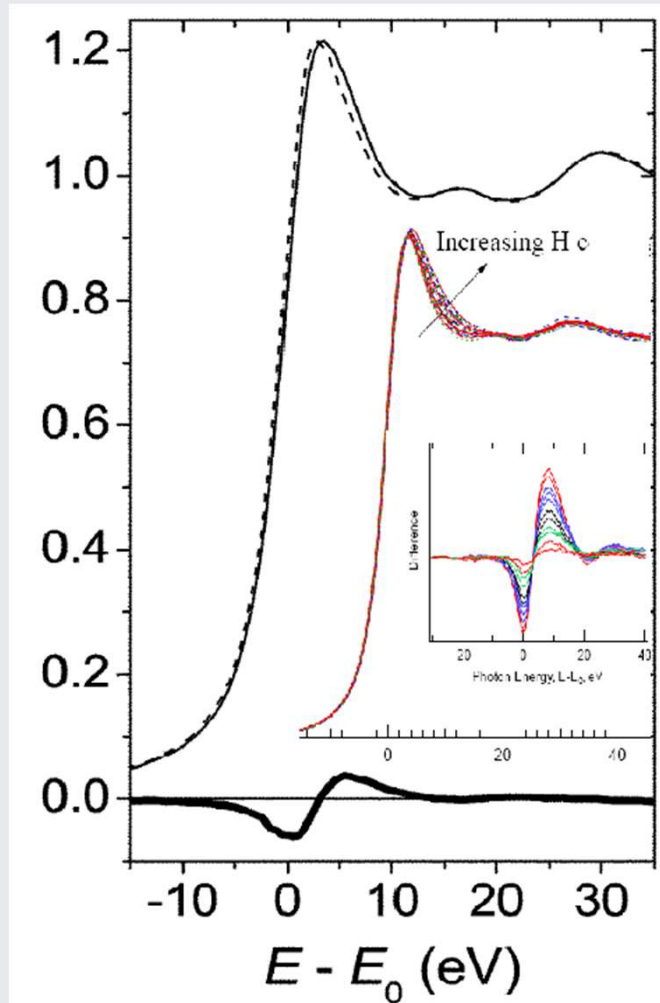


Melting of In μ -particles
and structure of
undercooled In phase



A. Filipponi et al. J. Synchr. Rad. 8, 81 (2001)

Time resolved & light elements XAS

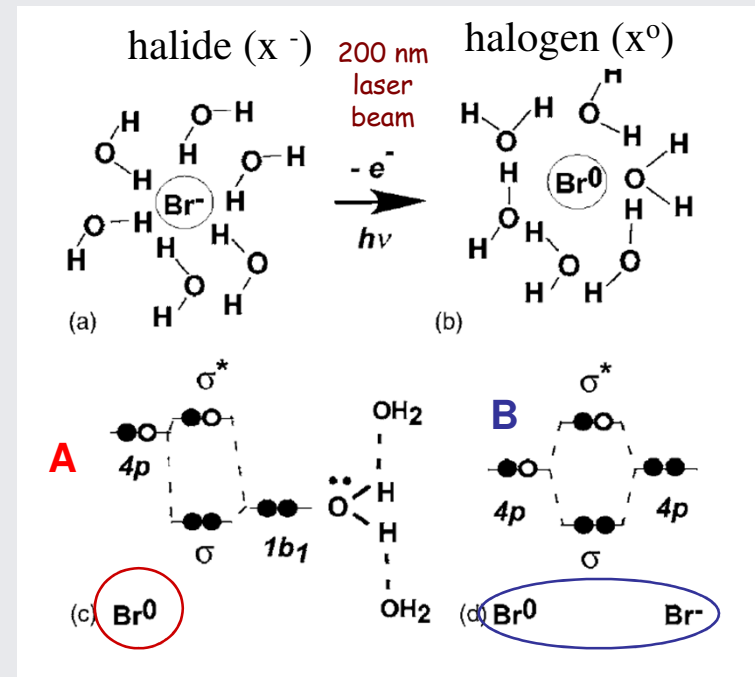
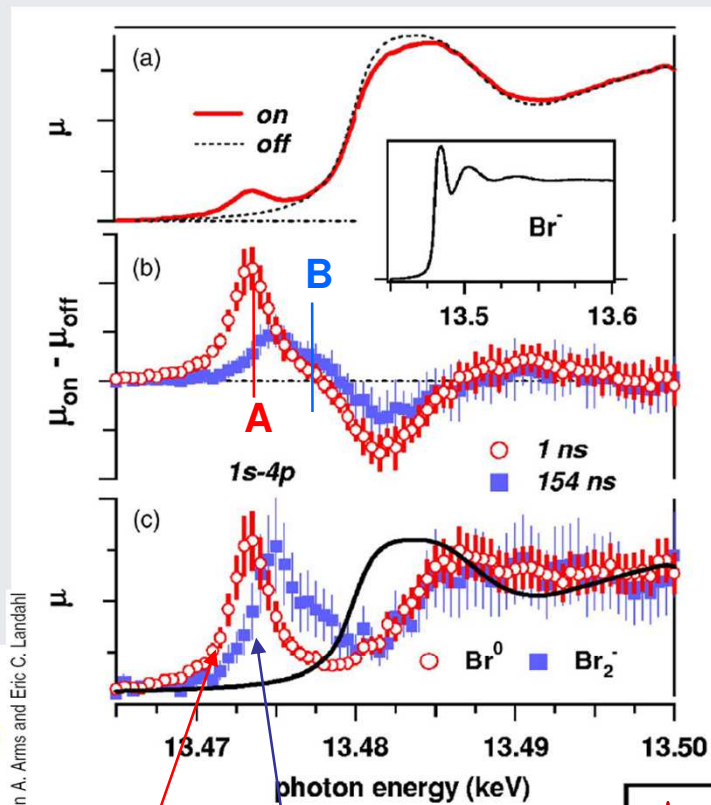


The Effect of H coverage on Pt nanoparticles:

H is notably weakly visible to x-ray but can be evident in the XANES region

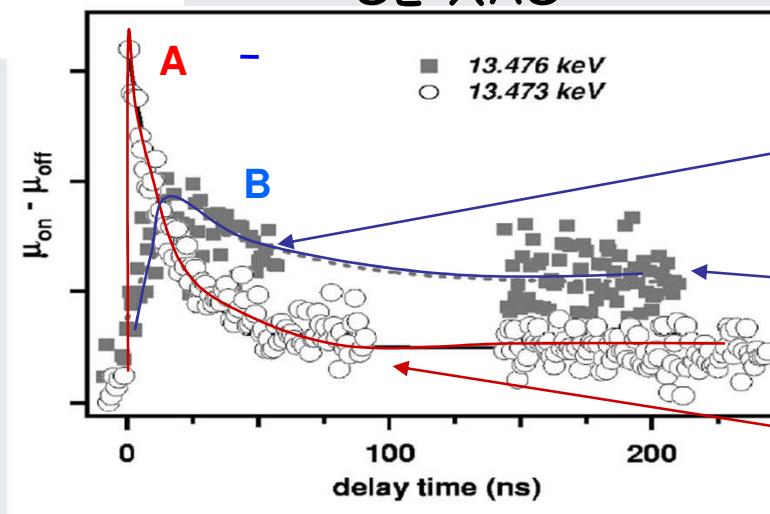
At the Pt L_{III} edge the effect of H is evident and can be followed in-situ to monitor the catalytic activity of Pt clusters as a function of environmental parameters.

Example: transient states of photoexcited hydrated atoms $\Delta t \sim 1$ ns



Br_0 Br_2^-

SE-XAS

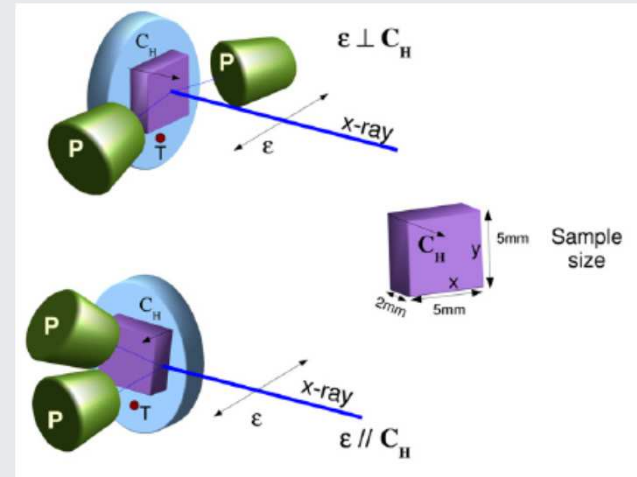
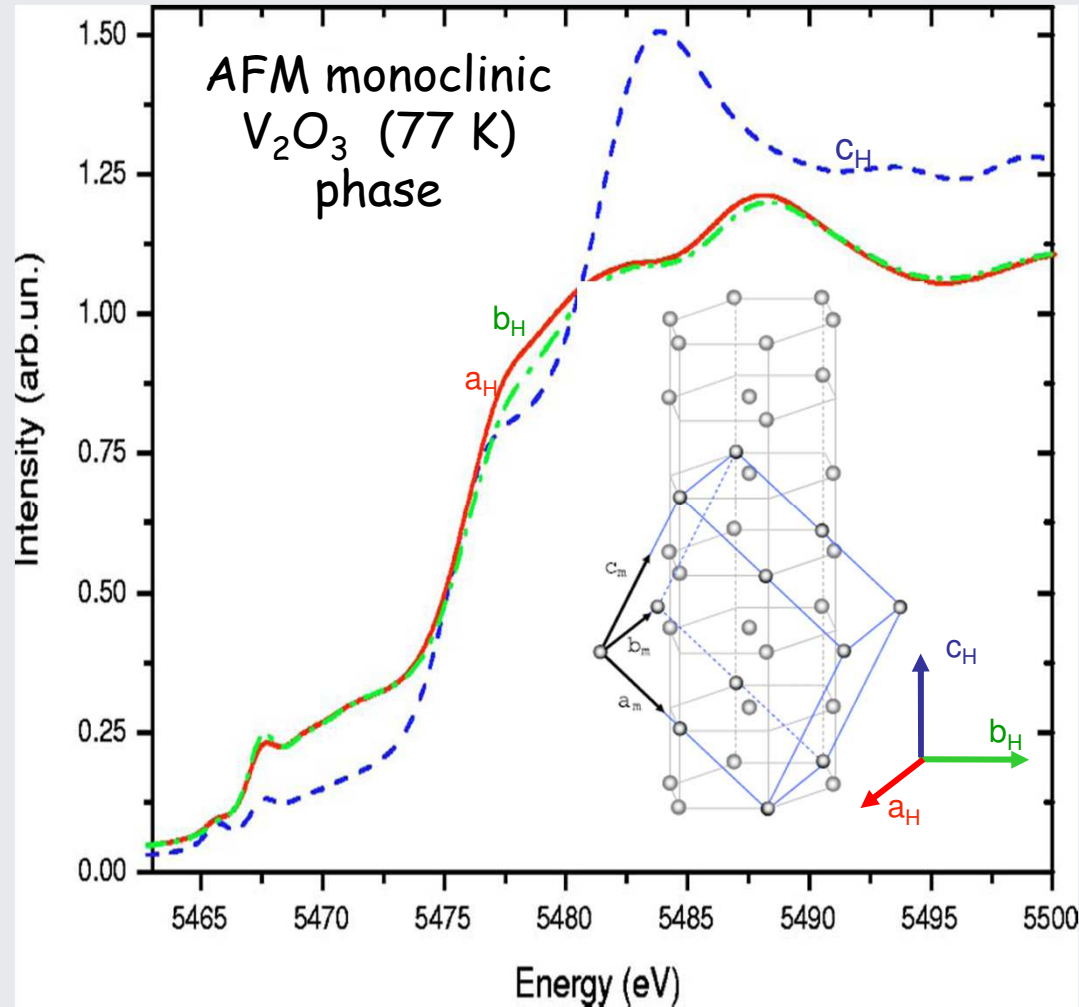


production of Br_2
($\Delta t \sim 10$ ns)

Br_2 molecules survive
after $\Delta t > 150$ ns

Reaction
with water
($\Delta t \sim 50$ ns)

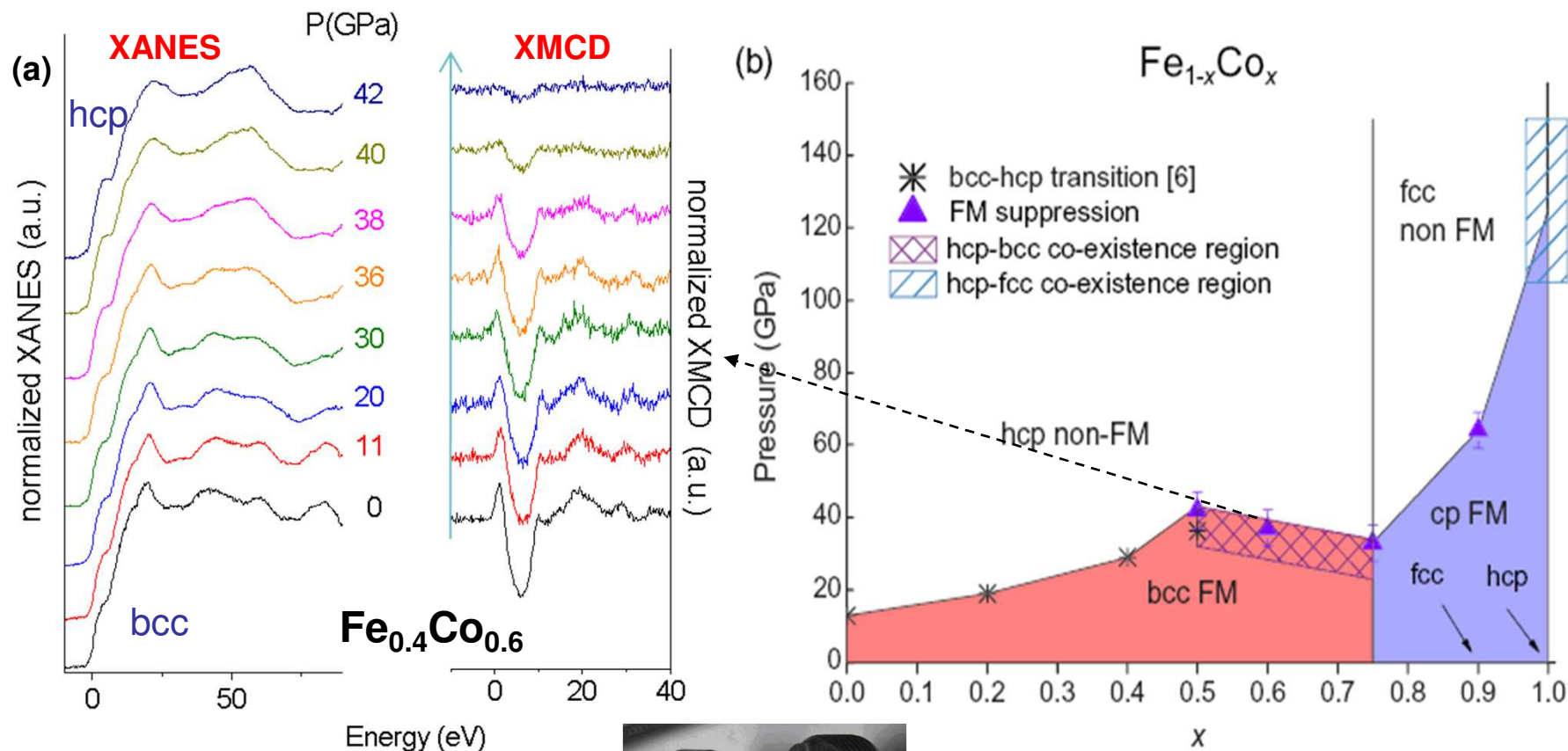
Polarized XANES: directional probe for not isotropic structures



Structural dichroism (absent in hexagonal HT phase) is the fingerprint of monoclinic distortion

XMCD-XANES extreme condition studies

High pressure structural and magnetic diagram of phase of 3d metal alloys



R. Torchio et al. High Pressure Research 31, 148-152 (2011)



Thanks for your attention